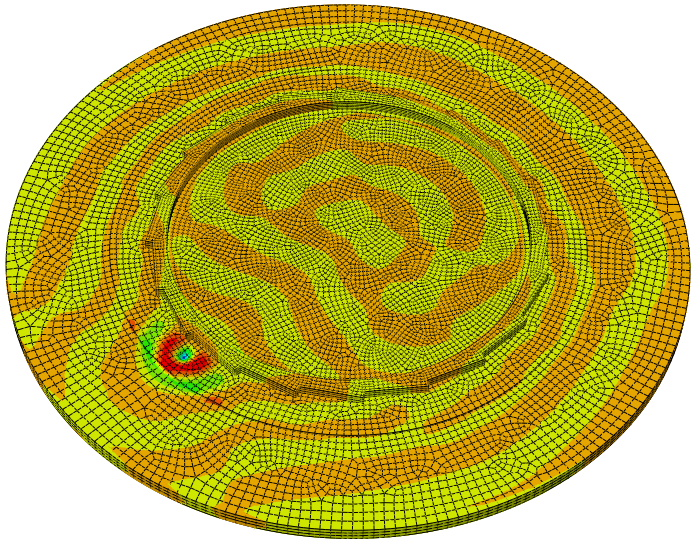

ANALYSIS OF VIBRATIONS IN HIGH-TECH FACILITY

PETER PERSSON

Structural Mechanics

Master's Dissertation

Department of Construction Sciences
Structural Mechanics

ISRN LUTVDG/TVSM--10/5164--SE (1-73)
ISSN 0281-6679

ANALYSIS OF VIBRATIONS IN HIGH-TECH FACILITY

Master's Dissertation by

PETER PERSSON

Supervisor:

PhD Kent Persson,
Div. of Structural Mechanics

Examiner:

Associate Professor Delphine Bard
Div. of Engineering Acoustics

Printed by Wallin & Dalholm Digital AB, Lund, Sweden, June, 2010 *(Pl)*.

For information, address:
Division of Structural Mechanics, LTH, Lund University, Box 118, SE-221 00 Lund, Sweden.
Homepage: http://www.byggmek.lth.se

Department of Construction Sciences
Structural Mechanics

ISRN LUTVDG/TVSM--10/5164--SE (1-73)
ISSN 0281-6679

ANALYSIS OF VIBRATIONS IN HIGH-TECH FACILITY

Master's Dissertation by

PETER PERSSON

Supervisor:

PhD Kent Persson,
Div. of Structural Mechanics

Examiner:

Associate Professor Delphine Bard
Div. of Engineering Acoustics

Printed by Wallin & Dalholm Digital AB, Lund, Sweden, June, 2010 *(Pl)*.

For information, address:
Division of Structural Mechanics, LTH, Lund University, Box 118, SE-221 00 Lund, Sweden.
Homepage: http://www.byggmek.lth.se

Preface

This master thesis was carried out at the Division of Structural Mechanics at LTH, Lund University, from October 2009 to May 2010.

First I would like to thank my supervisor Ph.D. Kent Persson, at the Division of Structural Mechanics, for his great guidance and support during this work. This master thesis would not have been possible without his help. I also would like to thank the staff at the Division of Structural Mechanics and the staff at MAX-lab for interesting and helpful discussions.

A special thanks to my father Ronny Persson for his great support and decisive engagement during my entire education.

Lund, May 2010

Peter Persson

Abstract

MAX-lab is a national synchrotron radiation facility in Lund. Nowadays, the MAX project consist of three facilities (three storage rings). A new storage ring is needed to improve material science, such as nanotechnology. MAX IV, also in Lund, will be 100 times more efficient than already existing synchrotron radiation facilities. The storage ring is controlled by a large number of magnets that are distributed along the ring. Since the quality of the measurement results from the MAX IV ring is dependent on the precision of the synchrotron light, a very strict requirement regarding the vibration levels of the magnets are defined. Vibration levels must be less than 26 nm during 1 s in the frequency span of 5-100 Hz. The site of MAX IV is located in an area in northeastern Lund called Brunnshög. At the site there is sedimentary bedrock and the soil mostly consists of boulder clay. The floor of the MAX IV building will mainly be constituted of a concrete structure. The inner and the outer radius of the structure are approximately 70 m and 110 m respectively and the storage ring has a circumference of approximately 500 m. The roof reaches the height of approximately 13 m.

The aim is to establish realistic finite element models that predict vibrations on the floor at the magnet foundation with high accuracy. The ultimate goal is to show how the structure can be constructed to reduce the vibration levels and to check the fulfilment of the requirements. Vibrations are analysed by the finite element method. Steady-state analyses are performed to investigate vibrations at the magnet foundations for varying parameters. Transient analyses are performed to compare the results with the requirements by using realistic walking loads.

The geometry of the FE-model was chosen to include the main laboratory concrete floor, the storage ring tunnel and the soil. Interfaces between building elements are assumed to have full interaction and since the structure is exposed to loads with low magnitude both the concrete and the soil were modeled as linear elastic isotropic materials.

A parameter study was performed to investigate the dynamic behavior of the structure. The load was applied as a harmonic concentrated force positioned on the floor, 10 m from the outer boundary. A frequency sweep in the range of 0-40 Hz was made to investigate the behavior of the structure at different load frequencies. It was concluded that the low stiffness of the soil was the main cause of the vibration levels of the magnet foundations in the storage ring tunnel. To simulate the walking load as realistic as possible, it was applied as a transient moving load. Analyses were made for two load patterns on the concrete floor corresponding to tangential and radial walking patterns. It was concluded that the vibration levels of the magnet foundations generated by the walking load of one person exceeds the requirements when walking next to the storage ring tunnel. Even if the walking load is located several meters away from the tunnel walking loads, especially from groups of people, must be considered in the design process.

Contents

1

Introduction

1.1 Background

MAX-lab is a national laboratory in Lund operated jointly by the Swedish Research Council and Lund University. Nowadays, the MAX project consist of three facilities (three storage rings): MAX I, MAX II, MAX III and one electron pre-accelerator called MAX Injector. In Figure 1.1 the present MAX-lab facility can be seen.

A new storage ring is needed to improve material science, such as nanotechnology. MAX IV, also in Lund, will be 100 times more efficient than already existing synchrotron radiation facilities, e.g. it is planned to be the next generation Swedish synchrotron radiation facility. MAX IV will basically consist of a main source that will be a 3 GeV ring with state-of-the-art low emittance for the production of soft and hard x-rays as well as an expansion into the free electron laser field. The second source will be the Linac injector, an underground tunnel next to the main ring. The Linac will provide short pulses to the main ring. In Figure 1.2 a 3D view of the MAX IV area can be seen.

In the storage ring the electrons are accelerated at high speeds. The particles then emit electromagnetic radiation, so-called synchrotron light. The storage ring is controlled by a large number of magnets that are distributed along the ring. The main concern is that vibrations at the magnets will give rise to a ten-fold increase of the vibration of the electron beam. Since the quality of the measurement results from the MAX IV ring is dependent on the precision of the synchrotron light, a very strict requirement regarding the vibration levels of the magnets are specified. The strict requirement is especially put on the mean vertical vibration level that must be less than 26 nm during one second in the frequency span of 5-100 Hz. Vibrations with frequencies lower than 5 Hz may be adjusted by an active calibration system. In the interval between 0-5 Hz vibration levels up to 260 nm are therefore

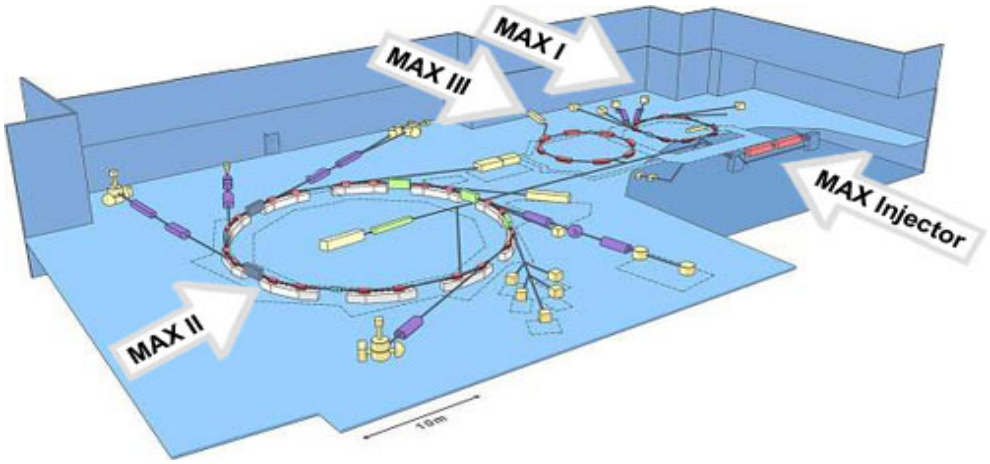

Figure 1.1: The present MAX-lab facility, [11].

allowed. Frequencies higher than 100 Hz may be neglected and probably have very low amplitudes since they are easily damped out in the structure.

In a facility like the MAX-lab, the structure is exposed to both harmonic and transient excitations. The harmonic excitations are typically working machines like pumps, ventilation and other electrical equipment. Transient excitations are typically traffic from the nearby roads and human activities in the building such as walking, closing doors and dropping objects.

The site of MAX IV is located in an area in northeastern Lund called Brunnshög. At the site there is sedimentary bedrock, shale. The soil at the site mostly consists of boulder clay with a varying thickness of 8-10 m. The floor of the MAX IV building will mainly be constituted of a concrete structure. The inner and the outer radius of the structure are approximately 70 m and 110 m respectively and the storage ring has an circumference of approximately 500 m. The roof reaches the height of approximately 13 m.

The floor plan of the MAX IV ring is shown in Figure 1.3 with its different cross-sections according to the serrated contours.

The MAX IV ring will have 20, equally distributed, experiment stations along the storage ring where the electrons are led out from the ring to the stations in strait beam lines according to Figure 1.4. This results in that the same segment is repeated 20 times.

In Figure 1.5 the most common cross-section of the proposed MAX IV ring building is shown. The section varies slightly according to the serrated outer wall of the storage ring tunnel and the serrated outer wall of the building. The cross-section where the storage ring meets the underground tunnel Linac is different from Figure 1.5 according to Figure 1.3.

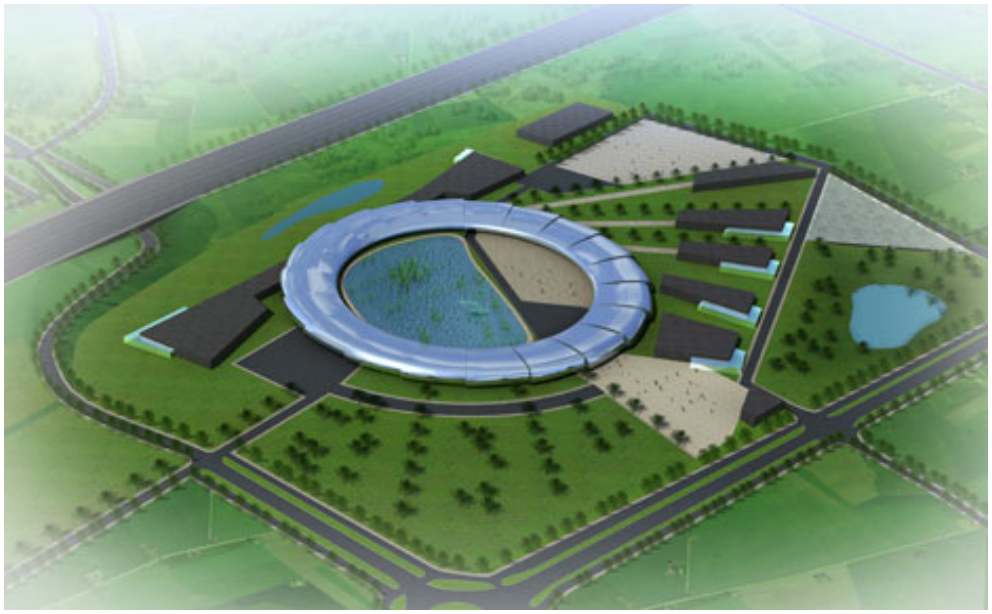

Figure 1.2: 3D view of MAX IV area, [11].

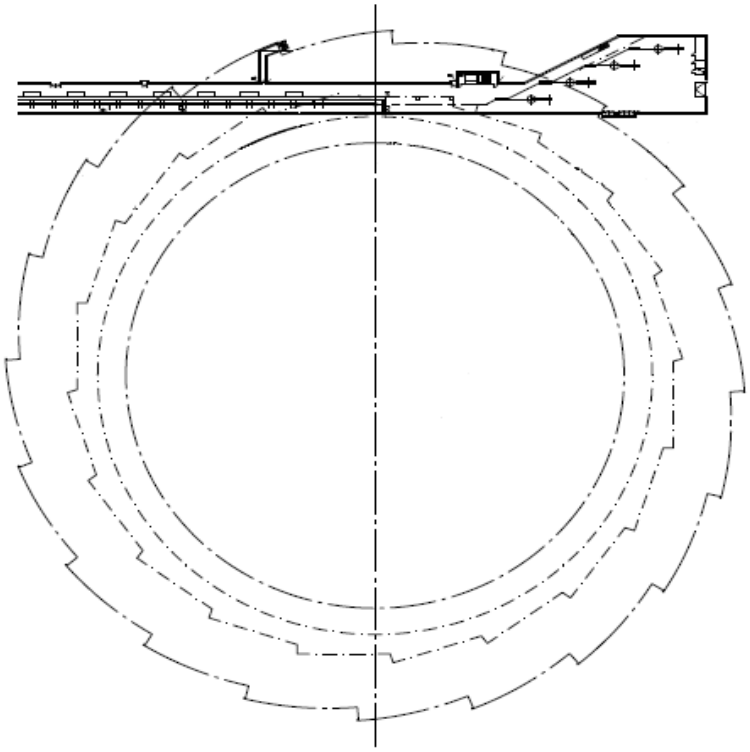

Figure 1.3: Floor plan of MAX IV ring, [12].

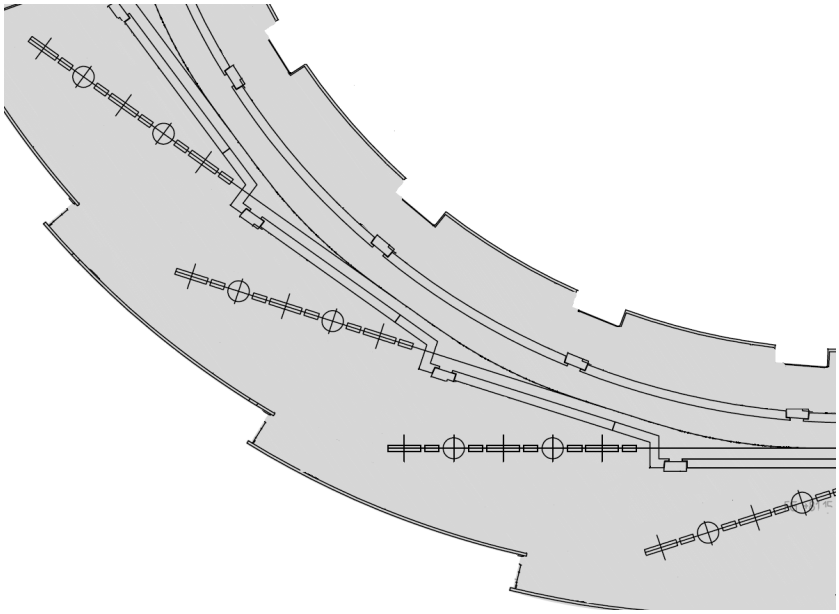

Figure 1.4: Detailed floor plan of MAX IV with beam lines, [12].

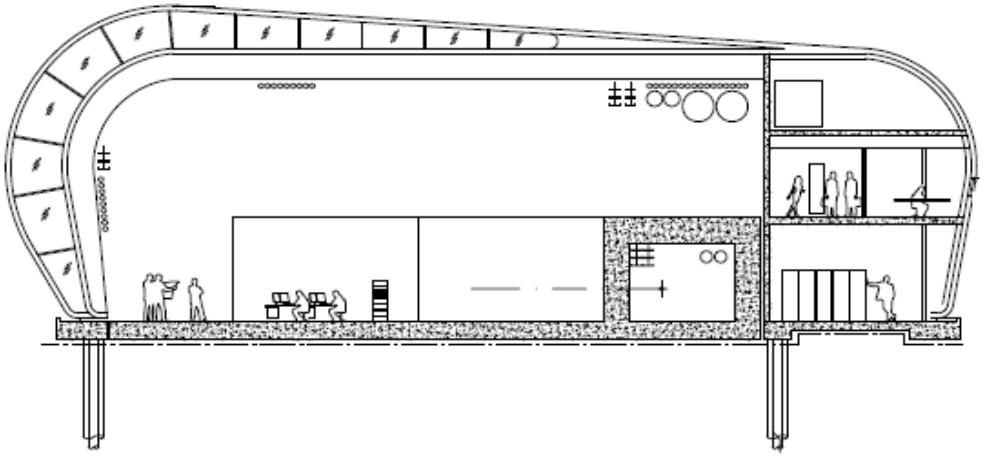

Figure 1.5: A section of the MAX IV ring, [12].

1.2 Objective and method

The main objective is to study the main floor and the tunnel regarding vibrations that may occur at the base of the magnet foundations in the storage ring due to different excitations. The aim is to establish realistic finite element models that predict vibrations of the magnets with high accuracy. The ultimate goal is to suggest a proper construction that minimize the vibration levels and to check the fulfilment of the requirements. The vibrations are analysed by use of the finite element method for both harmonic as well as transient loading situations.

1.3 Disposition

The report includes the following chapters;

- In chapter 2 the materials concrete and soil are generally described.
- In chapter 3 the introduction of the used vibration theories are treated.
- In chapter 4 an introduction to the finite element method is given.
- In chapter 5 the FE-model and the FE-modeling are described.
- In chapter 6 is the method described and the results presented and discussed for harmonic and transient loading.
- In chapter 7 discussion and suggestions for further work are presented.

2

Materials

2.1 Concrete

Concrete is a composite that mainly consists of cement, sand, aggregate and water. With different admixture the concrete can get various properties. When adding water it reacts with cement and the concrete gets hardened. The process is called hydration.

Hardened concrete has a density of 2400 kg/m^3 and a Poisson's ratio of 0.2 according to [1]. A list of the characteristic values for Young's modulus for classified concrete is presented in [1]. The characteristic value is the 5 % fractile of the statistical distribution. The values are in the range 27.0-39.0 GPa and is valid for static loading. For dynamic loading a multiplication factor of 1.2 should be used, [1]. The damping ratio for a concrete structure depends on the cracks, the joints, the reinforcement and the stress level. According to [3] the damping ratio for a concrete structure is in the range 2-10 % where the lower values corresponds to a well-reinforced concrete structure with low stress level and slight cracking. The most significant property of concrete is that the tensile strength is just about 1/10 of the compressive strength. Tensile stresses can lead to cracking because of the low tensile strength.

To prevent the concrete's tendency to crack, reinforcement is used. The reinforcement is usually several reinforcing bars of steel that are placed out before the concrete is casted. Forces are transferred between the concrete and the reinforcing bars by bonding and by contact pressure. There is also pre-stressed concrete where pre-stressed cables are used instead of or together with reinforcing bars. The pre-stressed cables contribute to an initial compressive stress of the concrete and therefore has a higher capacity.

Concrete is the dominating construction material and is used in areas such as houses, plants, bridges, piles and foundations, [4].

2.2 Soil

For more information about the material parameters of the soil and some of the facts in this section, see [5] and [6].

Moraine covers about 75 % of Sweden's land area and is the most common soil type in Sweden. How the moraine is graded depends on what kind of bedrock there was present when it was formed. The moraine was formed when the ice sheets retreated and erode the bedrock. In areas with sedimentary rocks, e.g. southwestern Scania, there is such a significant amount of clay that is regarded as clay and called boulder clay. In areas with harder bedrock the moraine is more coarsely graded.

Strength and deformation properties of soil are a broad area with many uncertainties because of its varying composition. Parameters describing the deformation properties of soil are often determined by laboratory tests and sometimes from in situ tests. Properties of moraine depend on the formation of the moraine and how the ice has packed it. Moraine is therefore an unsorted and coarsely graded soil with varying properties.

Moraine is a very firm soil with an undrained shear strength of over 100 kPa whereas for boulder clay the undrained shear strength may be about 200-300 kPa. The stress-strain curve for a soft clay usually shows a linear behavior up to the preconsolidation pressure and in the overconsolidated state soil has mainly an elastic response upon unloading. Therefore soil is usually assumed to be linear elastic in overconsolidated state, i.e. at pressures lower than the preconsolidation pressure. Heavily overconsolidated fine graded soil and well compacted coarse graded soil show mainly an elastic response in shearing when exposed to loads with low magnitude. The soil at the site of MAX IV is regarded as heavily overconcolidated due to the preconcolidation pressure is set to 400 kPa and it is exposed to vibration loads with low magnitude.

Clays often have a very low hydraulic conductivity i.e. its take time for clays to drain water during loading. Therefore the drained shear strength is only used when it concerns long term loading, which implies that the undrained shear strength is used for the temporary loads such as traffic, walking and impact.

Clays are usually water saturated. This results in that the density is the same for natural moisture clay as water-saturated clay. The density for a clay is normally between 1400 and 2000 kg/m^3 and for a boulder clay the density should be closer to 2000 kg/m^3 because it is a coarsely graded soil. Since the clay normally is water-saturated and water is incompressible the Poisson's ratio is often set to 0.5. The damping for soil, in this case boulder clay, is strain-dependent, i.e. the damping increases with the strain. Therefore the damping is set higher for earthquake analysis than for analysis of very small vibration levels. The damping ratio could vary from around 1 to around 20 %.

3

Vibration Theory

3.1 Introduction

Vibrations occur in every building due to various kinds of loading. These loads vary in time and cause vibrations. There is a big difference between static and dynamic problems. For static problems the solution follows the natural intuition, a bigger load needs a heavier structure to support the loads. For dynamic problems the frequency of the load needs to be taken into account. If the frequency of the load is close to a natural frequency of the system the displacements will become much greater than if the frequency of the load is far from a natural frequency.

A dynamic event may be plotted in time domain or in frequency domain. In the time domain the system is described as time dependent and in the frequency domain the system is described as frequency dependent. To convert a signal in the time domain to the frequency domain and vice versa, a "Fast Fourier Transform (FFT)" algorithm can be used.

The easiest way to describe a dynamic system is by use of a single-degree of freedom model, SDOF. An SDOF only contains one DOF meaning that it only needs one DOF to describe the exact position of the mass. The system shown in Figure 3.2 consists of a mass, a damper and a spring. The mass, m, is to be located in a point and the displacement, u, is in one direction. The load $p(t)$ is a time-dependent loading. The damper and the spring are regarded as mass-less.

Force equilibrium and Newton's second law gives

$$p(t) - c\dot{u} - ku = m\ddot{u} \tag{3.1}$$

and rewriting it to the equation of motion of a SDOF model

$$m\ddot{u} + c\dot{u} + ku = p(t) \tag{3.2}$$

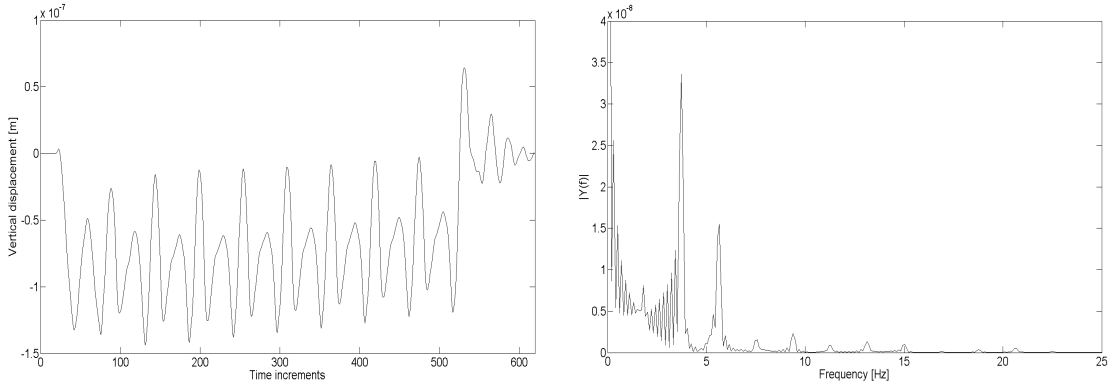

(a) Time domain. (b) Frequency domain.

Figure 3.1: Example of plotting result in different domains.

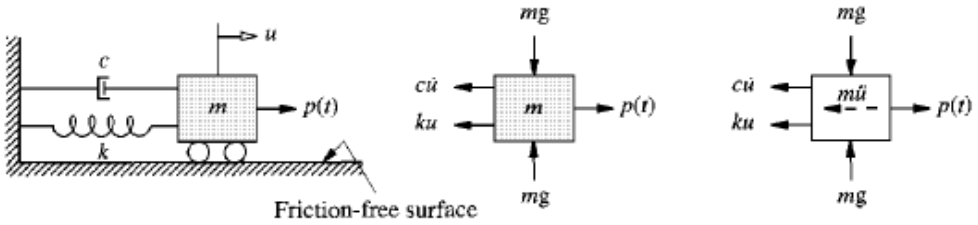

Figure 3.2: Single-degree of freedom model, [3].

To describe motion of a more complex structure a multi-degree of freedom model is used, MDOF. In an MDOF system the number of DOFs is proportional to the number of finite elements in the FE-model. To generate more accurate result more DOFs in the model must be considered.

The equation of motion for a MDOF system is

$$\mathbf{M\ddot{u} + C\dot{u} + Ku = P(t)} \tag{3.3}$$

where $\mathbf{M}$ is the mass matrix, $\mathbf{C}$ is the damping matrix, $\mathbf{K}$ is the stiffness matrix, $\mathbf{P}(\mathrm{t})$ is the applied force vector and $\mathbf{u}$ is the displacement vector.

3.2 Natural frequencies and mode shapes

A structure has an unlimited number of natural frequencies, i.e. unlimited number of degrees of freedom. In a finite element model there is equal number of natural frequencies as number of degrees of freedom.

If a structure is excited with a frequency near the natural frequency the amplitude will significant increase. This is called resonance. If there are not any damping

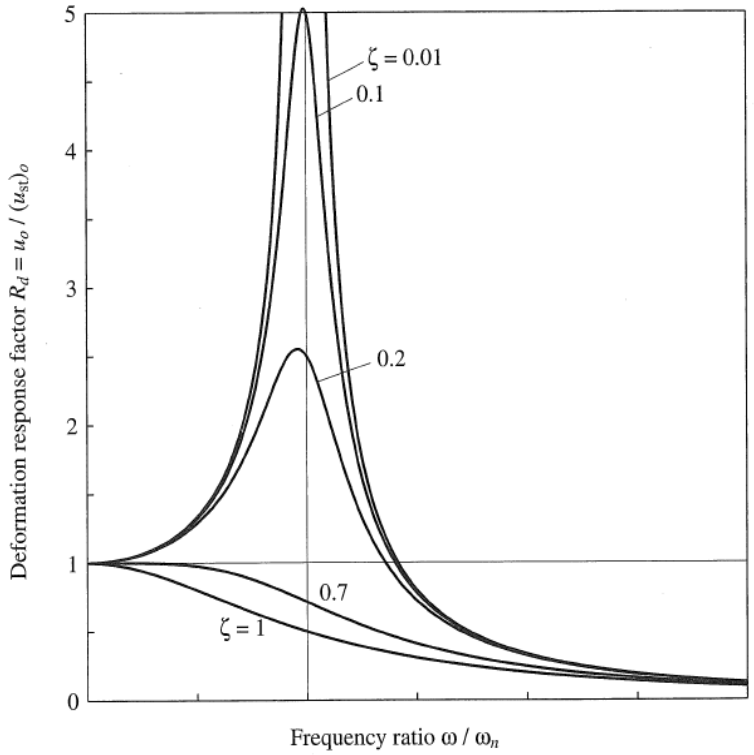

Figure 3.3: Deformation response factor for a damped system excited by harmonic force, [3].

present in the structure the amplitude will be infinite, but there is always damping present in a structure.

The vertical axis shows the deformation response factor, R_d, that is the ratio between the dynamic and the static displacement. The horizontal axis shows the ratio between actual and the natural frequency.

For each natural frequency there is a corresponding deformation shape of the structure, mode shape. To determine the natural frequencies and the corresponding mode shapes a structure with negligible damping is considered.

The equation of motion of an undamped system with $\mathbf{p}(t)=0$ is

$$\mathbf{M\ddot{u} + Ku = 0} \tag{3.4}$$

The solution $\mathbf{u}(t)$ has to satisfied the initial conditions

$$\mathbf{u} = \mathbf{u}(0) \qquad \mathbf{\dot{u}} = \mathbf{\dot{u}}(0) \tag{3.5}$$

at t=0.

The free vibration of an undamped system, in one of the mode shapes, can be written

as

$$\mathbf{u}(t) = q_n(t)\phi_n \tag{3.6}$$

where $q_n(t)$ is time dependent and described by the harmonic function

$$q_n(t) = A_n cos\omega_n t + B_n sin\omega_n t \tag{3.7}$$

and ϕ_n represents the mode shapes and does not vary with time.

If $q_n(t)$=0 there is no motion of the system because it implies that $\mathbf{u}$(t)=$\mathbf{0}$. Therefore must ϕ_n and ω_n satisfy the eigenvalue problem

$$(-\omega_n^2\mathbf{M} + \mathbf{K})\phi_n = \mathbf{0} \tag{3.8}$$

If ϕ_n=0 there is no motion of the system according to previous argument. The solution gives the natural frequencies $\omega_1, ..., \omega_n$ where n is the number of DOFs. When the natural frequencies are known the natural modes ϕ_n can be calculated by using the eigenvalue problem, Eq.(3.8).

The natural frequencies are a property of the structure. For an undamped system the natural frequencies depend on the mass and the stiffness of the structure, both the value and the distribution. The natural frequencies of a damped system also depend on the damping ratio, ζ, according to Eq.(3.9), [3].

$$\omega_D = \omega_n\sqrt{1-\zeta^2} \tag{3.9}$$

3.3 Steady-State

The response of a system to harmonic excitation is common in structural dynamics and includes the concept steady-state vibration. Understanding the response of the system to harmonic excitation will provide insight into how the system will respond to other types of excitations, [3].

When a structure is excited by a force with the amplitude p_0 and the frequency ω an harmonic vibration occurs with the motion of equation

$$\mathbf{M\ddot{u}} + \mathbf{C\dot{u}} + \mathbf{Ku} = p_0 sin\omega t \tag{3.10}$$

The solution consists of a complementary solution and a particular solution. With the initial conditions, no initial displacement and no initial speed

$$u = u(0) \qquad \dot{\mathrm{u}} = \dot{\mathrm{u}}(0) \tag{3.11}$$

the particular solution is

$$u_p(t) = Csin\omega t + Dcos\omega t \tag{3.12}$$

and the complementary solution is

$$u_c(t) = e^{-\xi\omega_n t}(Acos\omega_D t + Bsin\omega_D t) \tag{3.13}$$

where A, B, C and D are integration constants.

The complete solution is then

$$u(t) = u_c(t) + u_p(t) = e^{-\xi\omega_n t}(Acos\omega_D t + Bsin\omega_D t) + Csin\omega t + Dcos\omega t \tag{3.14}$$

The solution contains two vibration components; transient vibration (complementary solution) and steady-state vibration (particular solution). The transient vibration decays exponentially with time towards zero. Then will only the steady-state vibration remains.

3.4 Determine damping

Damping is an effect that tends to reduce the vibration response in a structure. Damping is always present in a structure and arises for example from internal material damping and from friction in cracks and joints. Damping has a significant influence on the response of a structure exposed to a dynamic force.

The damping properties cannot be calculated and should therefor be determined using measurements from similar structures. If there are not any appropriate measurements the damping matrix can be determined with different procedures using damping ratios.

3.4.1 Rayleigh damping

For further reading about the Rayleigh damping method and for reference, see for example [3].

Classical damping is an appropriate idealization if the mass and stiffness are evenly distributed through the structure. Rayleigh damping is a procedure to determine the classical damping matrix with the use of damping ratios. It consists of two parts; one is presupposing mass-proportionality and the other one is presupposing

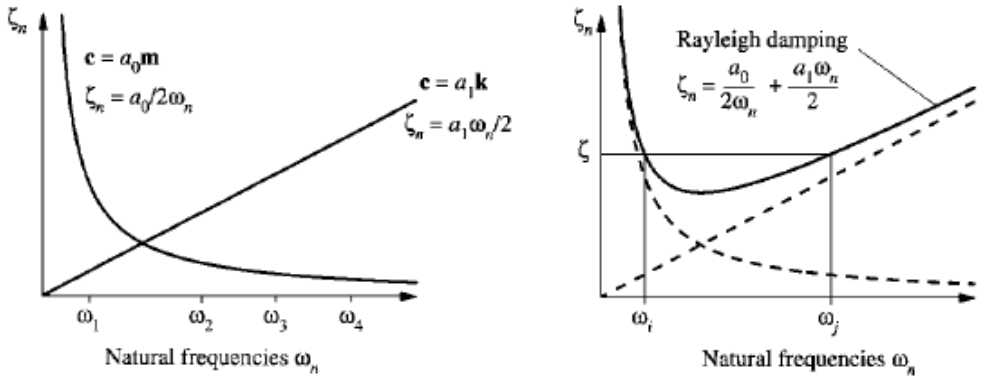

Figure 3.4: Rayleigh damping, [3].

stiffness-proportionality, according to Eq.(3.15). This has no physical basis but it is proved to be a good approximation.

$$\mathbf{c} = a_0\mathbf{m} + a_1\mathbf{k} \tag{3.15}$$

The damping ratio for the nth mode is

$$\zeta_n = \frac{a_0}{2}\frac{1}{\omega_n} + \frac{a_1}{2}\omega_n \tag{3.16}$$

In Rayleigh damping the damping ratio, ζ, is used to describe the influence of damping. The damping ratio is dimensionless and is the ratio between the damping constant, c, and the critical damping coefficient, c_{cr}, according to Eq.(3.17).

$$\zeta = \frac{c}{c_{cr}} \tag{3.17}$$

For buildings the damping ratio is normally less than 1 which means that the system is underdamped. If the damping ratio is equal to 1 the system is critically damped and for damping ratios greater than 1 the system is overdamped.

If the damping ratios ζ_i and ζ_j can be assumed to have the same value the coefficients a_0 and a_1 can be written as

$$a_0 = \zeta\frac{2\omega_i\omega_j}{\omega_i + \omega_j} \qquad and \qquad a_1 = \zeta\frac{2}{\omega_i + \omega_j} \tag{3.18}$$

where ζ is the damping ratio. ω_i and ω_j determine the frequency range where the damping ratio is valid.

In Figure 3.4 it is shown that the mass damps the lower frequencies and the stiffness damps the higher frequencies.

A soil-structure system is an example of a system with two or more parts with significantly different damping ratios. The assumption of classical damping is not appropriate for this kind of systems but it is appropriate for each part separately. The damping matrix for the system, nonclassical damping matrix, is constructed by assembling the two classical damping matrixes, one for each part. It is appropriate to use Rayleigh damping for each part.

3.5 Wavelength

The wavelength is the distance over which the shape of the wave repeats itself.

The bending wave number for an isotropic plate is given by [13] as

$$k = (\frac{\omega^2 \rho h}{EI})^{\frac{1}{4}} \tag{3.19}$$

where ω is the angular frequency, ρ is the density, h is the height of the plate and EI is the bending stiffness of the cross-section.

The bending wave number is also given by

$$k = \frac{2\pi}{\omega} = \frac{\omega}{c} \tag{3.20}$$

Combining Eq.(3.19) and Eq.(3.20) the bending wave speed in an isotropic plate is given as

$$c = \sqrt{\omega} \sqrt[4]{\frac{EI}{\rho h}} \tag{3.21}$$

The wave speed of a shear wave in an isotropic material is given by

$$c = \sqrt{\frac{G}{\rho}} \tag{3.22}$$

whereas the wave speed of a surface wave in an isotropic material is given by

$$c = \sqrt{\frac{E}{\rho}} \tag{3.23}$$

The relation between the wave speed, c, and the wavelength, λ is given by

$$\lambda = \frac{c}{f} \tag{3.24}$$

where f is the frequency.

3.6 RMS-value

RMS stands for Root Mean Square and is used as a measure of the magnitude of a vibration. This is used instead of the mean value since the sign of the displacements may change during an analysis.

$$u_{RMS} = \sqrt{\frac{1}{\Delta t}\int_{t_0}^{t_0+\Delta t} u^2(t)dt} \tag{3.25}$$

where u is the displacement amplitude and t is the time.

4

The Finite Element Method

For further reading about the finite element method and for reference, see for example [2].

Differential equations are often used to describe various physical problems. Sometimes differential equations are too complicated to be solved analytically instead numerical methods are required. Such a method is the finite element method, FEM, that solves arbitrary boundary valued differential equations with arbitrary geometries and materials.

Development of FEM took off in early 1960's and FEM is currently the most effective method for solving arbitrary differential equations in engineering, physics and mathematics. In order to solve differential equations with FEM the body is divided into small elements, finite elements. In FEM the variables of each element is approximated. The body with the finite elements is called a finite element mesh. Every element has a relatively simple approximation, often a polynomial. At some points in the element the variables must be known, often at the boundary.

Since it is often tens of thousands of unknown degrees of freedom, the system of equations cannot be solved without computer calculations. A finer mesh, an therefore an increased amount of DOFs, will normally generate a more accurate solution.

4.1 Isoparametric finite elements

When modelling bodies with arbitrary geometries the finite elements must be allowed to have curved boundaries, i.e. general shapes. Consider a cubic region in a local $\xi\eta\zeta$-coordinate system that is bounded by $\xi=\pm\ 1$, $\eta=\pm\ 1$ and $\zeta=\pm\ 1$. The local region is called the parent domain. This simple geometric shape in the local coordinate system is mapped, transformed, into more a more complex geometry in

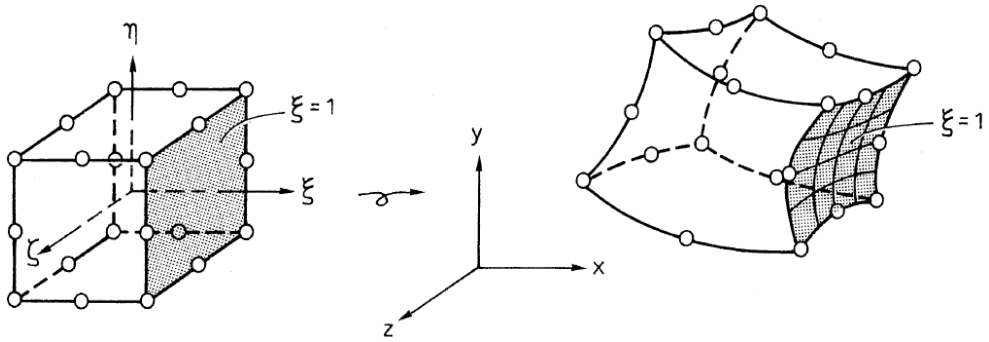

Figure 4.1: Mapping of a 20-node 3D isoparametric element, [2].

the global Cartesian xyz-coordinate system. The global region is called the global domain. See Figure 4.1.

For every point in the $\xi\eta\zeta$-coordinate system there is a corresponding point in the xyz-coordinate system. The mapping is therefor described by

$$x = x(\xi, \eta, \zeta); y = y(\xi, \eta, \zeta); z = z(\xi, \eta, \zeta) \tag{4.1}$$

Differentiate Eq.(4.1) and use the chain rule of partial differentiation to obtain

$$\begin{bmatrix} dx \\ dy \\ dz \end{bmatrix} = \begin{bmatrix} \frac{\partial x}{\partial \xi} & \frac{\partial x}{\partial \eta} & \frac{\partial x}{\partial \zeta} \\ \frac{\partial y}{\partial \xi} & \frac{\partial y}{\partial \eta} & \frac{\partial y}{\partial \zeta} \\ \frac{\partial z}{\partial \xi} & \frac{\partial z}{\partial \eta} & \frac{\partial z}{\partial \zeta} \end{bmatrix} \begin{bmatrix} d\xi \\ d\eta \\ d\zeta \end{bmatrix} \tag{4.2}$$

The Jacobian matrix, $\mathbf{J}$, related to the mapping in Eq.(4.1) is defined by

$$\mathbf{J} = \begin{bmatrix} \frac{\partial x}{\partial \xi} & \frac{\partial x}{\partial \eta} & \frac{\partial x}{\partial \zeta} \\ \frac{\partial y}{\partial \xi} & \frac{\partial y}{\partial \eta} & \frac{\partial y}{\partial \zeta} \\ \frac{\partial z}{\partial \xi} & \frac{\partial z}{\partial \eta} & \frac{\partial z}{\partial \zeta} \end{bmatrix} \tag{4.3}$$

According to Eq.(4.2) any values of dξ, dη and dζ uniquely determine dx, dy and dz. To determine dξ, dη and dζ if the values of dx, dy and dz are given the transformation uses the inverted Jacobian matrix according to

$$\begin{bmatrix} d\xi \\ d\eta \\ d\zeta \end{bmatrix} = \mathbf{J}^{-1} \begin{bmatrix} dx \\ dy \\ dz \end{bmatrix} \tag{4.4}$$

Even if the mapping is unique it is not obtainable in the general case to invert Eq.(4.1) into the explicit forms of $\xi = \xi(x, y, z)$, $\eta = \eta(x, y, z)$ and $\zeta = \zeta(x, y, z)$.

To fulfill the convergence requirement the compatibility and the completeness requirement must be satisfied. If the element behaves compatible in the parent domain it will also do so in the global domain and the adjacent elements will match appropriately. The completeness requirement is satisfied if the sum of all values of the element shape function at every node in the element is equal to 1, according to Eq.(4.5).

$$\sum_{i=1}^{n} N_i^e = 1 \tag{4.5}$$

To map an element from the parent domain to a global domain requires that the nodes on one element boundary in the parent domain also are located on one element boundary in the global domain. It also requires that a corner node in one domain must correspond to a corner node in the other domain, this also include the mid-side nodes.

5

FE Model

5.1 Software

The finite element software *Abaqus* was used for the finite element calculations. *Abaqus* is divided into three parts; *Abaqus/CAE*, *Abaqus/Standard* and *Abaqus/Explicit*.

Abaqus/CAE is a user interface for modeling and meshing a structure and to visualize the results. *Abaqus/Standard* is an implicit solver for various dynamic finite element problems such as low-speed or steady-state analyses. *Abaqus/Standard* is also used for static problems. *Abaqus/Explicit* use the explicit method and is more appropriate for high-speed, nonlinear and transient response analyses.

In this investigation *Abaqus/CAE* was used for pre- and post processing and *Abaqus/Standard* for the analyses.

5.2 Geometry

The geometry of the FE-model was chosen to include the main laboratory concrete floor, the storage ring tunnel and the soil covering a radius of 150 m with a depth of 6 m. In Figure 5.1 a segment of the FE-model is shown. The segment is 1/20 of the whole model and this segment is repeated 20 times to produce the whole model.

The cross-section of MAX IV, shown in Figure 1.5, was somewhat simplified to just incorporate the main floor and the storage ring tunnel according to Figure 5.2. The outer wall of the storage ring tunnel is still serrated as shown in Figure 1.3. The dimension A shown in Figure 5.2 will therefore vary from 6-8 m.

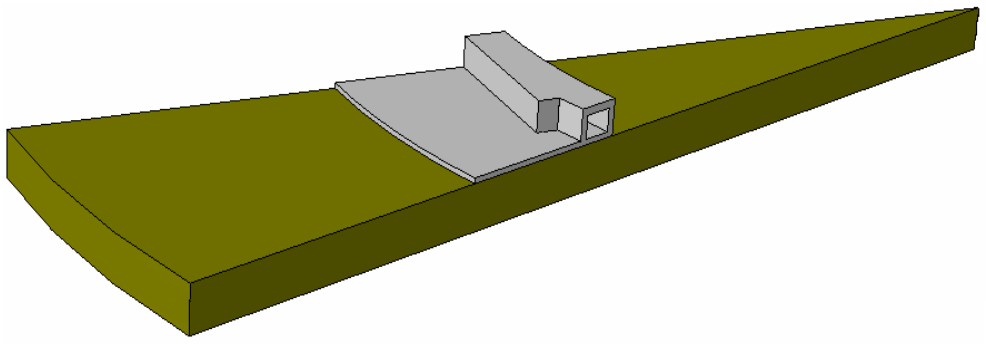

Figure 5.1: Segment of the FE-model.

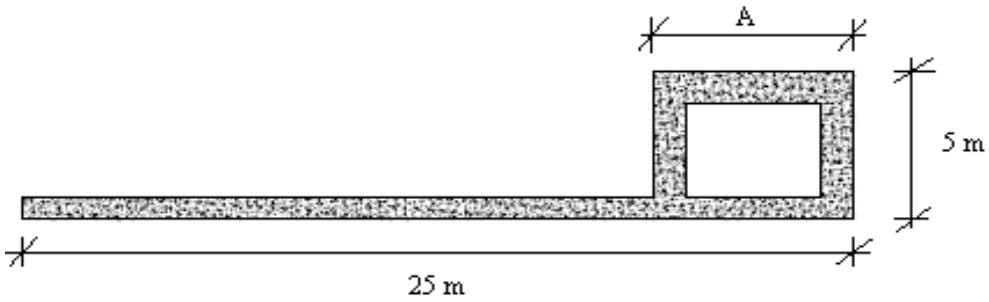

Figure 5.2: Simplyfied section of the concrete structure.

The dimensions of the simplified section were based on the architectural drawings. The inner and the outer radius of the modeled floor were 80 m and 105 m, respectively. The radius of the storage ring was 83 m. The base thickness of the floor was 700 mm and the thickness of the walls of the storage ring tunnel was 1000 mm.

5.3 Mesh

The model was meshed with 36 761 3D-solid elements ending up at 572 178 degrees of freedom. The mesh of the soil was coarser than that of the concrete structure.

5.3.1 3D-solid element

3D-solid isoparametric elements were employed in the model. The elements were 20-node quadratic brick elements, that is named $C3D20R$ in *Abaqus*. C stands for continuum stress/displacement, $3D$ means that it is a tree-dimensional element, 20 is the number of nodes and R means that reduced integration is used, [9]. Reduced integration means that the order of integration is lower than when full integration is used. Full integration provides a structure that is too stiff and therefore the

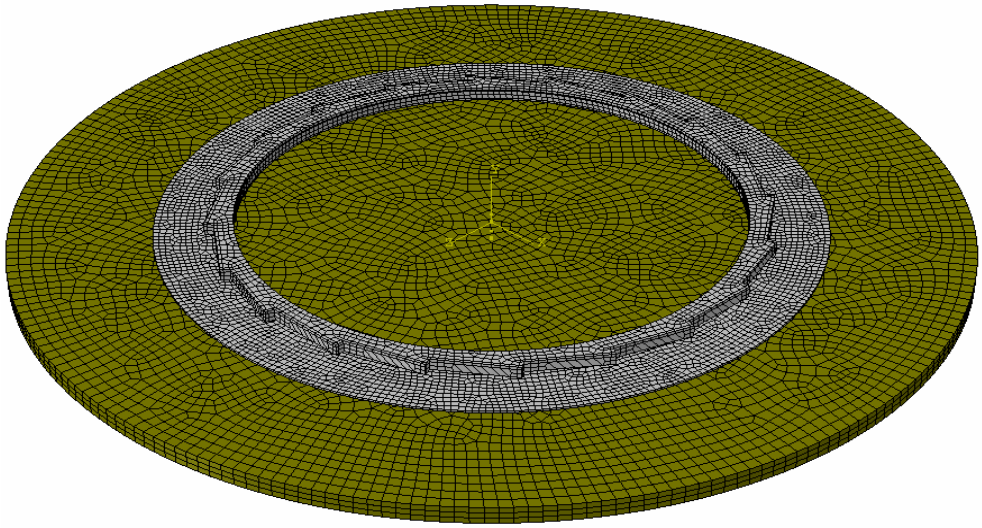

Figure 5.3: The mesh of the entire model.

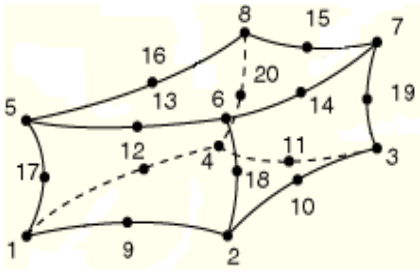

Figure 5.4: 20-node 3D-solid element, [9].

reduced integration may generate a more accurate solution, [2]. These elements only have translation degrees of freedom, in all three directions, and they use quadratic interpolation.

A convergences test was performed to evaluate how many elements needed in the thickness direction of the concrete floor. The investigation showed that only one element of the type $C3D20R$ was needed in the thickness direction.

To get a reliable output from a dynamic analyses, at least six nodes per wave length are needed. This implies for the quadratic element that the wave length must not be shorter than 2.5 elements, [9]. It is the wave length at the frequencies that generate the highest amplitudes that -is of interest, which for the present case are about 0-10 Hz. The maximum element size for the soil, regarding the wave length, is then 6 m. Due to the low frequencies that is of interest the wave length is not going to determine the element size for the concrete because concrete is significant stiffer than soil. Normally, a finer mesh will generate an more accurate solution but the computational cost will increase. To get a reasonable amount of elements the element size for the soil and the concrete is determined by the previous arguments.

5.4 Materials

Since the structure is exposed to loads with low magnitude both the concrete and the soil were modeled as linear elastic isotropic materials. Interfaces between building elements and between the structure and the soil are assumed to have full interaction. This means that the interfaces don't have any relative motion between them. A set of base material parameters is specified for the concrete and for the soil. The parameters are the Young's modulus, E, the Poisson's ratio, ν, the density, ρ, and the damping ratio, ζ.

5.4.1 Concrete

The density was set to 2400 kg/m^3 for the concrete. The Young's modulus was set to 40 GPa corresponding to the concrete type C 32/40 taking into account the dynamic addition of 20 % and the Poisson's ratio was set to the recommended value 0.2, according to [1]. The structure is exposed to loads with a low magnitude, i.e. working stress, the concrete was assumed to only be slightly cracked and the structure only has few joints. Therefore the initial value of the damping ratio was set to 2 %. Table 5.1 summarize the base material parameters for the concrete.

Table 5.1: *The base material parameter for the concrete.*

E	ν	ρ	ζ
40 GPa	0.2	2400 kg/m^3	2 %

5.4.2 Soil

The Young's modulus of the soil was assumed to vary with the depth. Therefore the soil was divided into three layers with equal thickness and varying Young's modulus. The equation for the variation of the Young's modulus with the depth was given by [14] to

$$E(z) = 22 + 5z \qquad [\text{MPa}] \tag{5.1}$$

The top 2 m soil is assumed to be excavated and replaced by the building. The Young's modulus for each layer was evaluated at the midpoint location. The density for boulder clay was set to 1800 kg/m^3 and was assumed to not vary with the depth. Due to choosing an elastic isotropic material, the Poisson's ratio was set to 0.45, close to being an incompressible material. The strain dependency of the damping ratio normally make it necessary to consider different damping ratios for different load magnitudes. In this study the base value was set to 20 % but other values were

also investigated. Table 5.2 summarize the base material parameters for the three layers of soil.

Table 5.2: *The base material parameter for the soil.*

Layer	E	ν	ρ	ζ
1	37 MPa	0.45	1800 kg/m^3	20 %
2	47 MPa	0.45	1800 kg/m^3	20 %
3	57 MPa	0.45	1800 kg/m^3	20 %

The sedimentary bedrock, shale, beneath the soil was regarded as infinite stiff. Consequently the bottom soil surface was constrained in the vertical direction. Moreover, in the horizontal directions only the rigid body motions were constrained.

5.4.3 Rayleigh damping

By choosing Rayleigh damping, the damping ratio varies with the frequency according to Eq.(3.16). To determine constant values for the coefficients a_0 and a_1 for all frequencies of interest, an approximation was made. The frequencies of interest were primarily assumed to be in the range 5-25 Hz. This is where the highest displacement amplitudes is expected to occur. The range was determined by studying the plots of the vertical displacement versus frequency, with various parameters, see Appendix A. A tolerance for the varying damping ratio was set to $\pm$ 15 % of the value for the damping ratio. In Figure 5.5 the frequency range of interest and the tolerance of the damping ratio are shown as dashed lines.

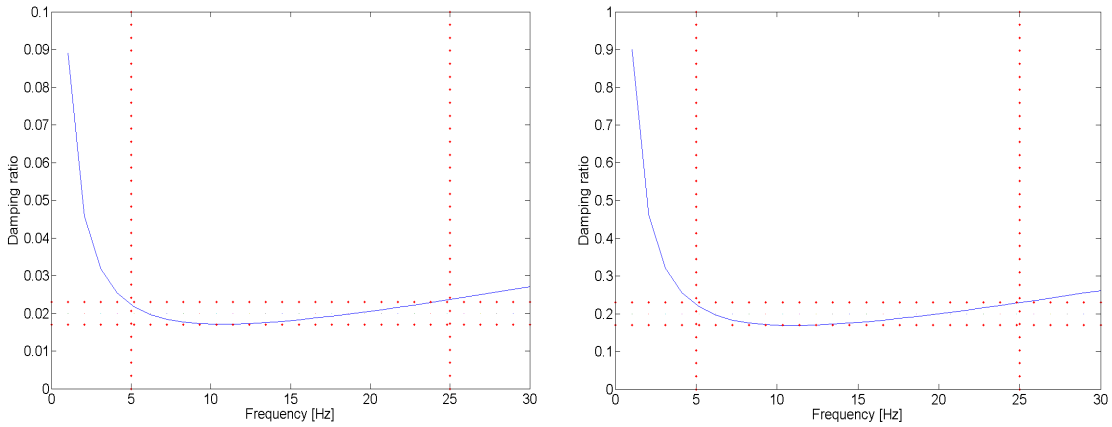

(a) Damping ratio for concrete, $\zeta = 0.02$.

(b) Damping ratio for soil, $\zeta = 0.20$.

Figure 5.5: Rayleigh damping.

By choosing a certain damping ratio the damping ratio versus frequency may be plotted. Figures in Figure 5.5 show plots of the damping ratio versus frequency for the base values for both concrete and soil.

5.5 Loading

The structure was analysed for two types of dynamic loads. In the Harmonic loading chapter sinusoidal harmonic concentrated loading was applied and in the Transient loading chapter transient walking loads was applied.

6

Modelling Results

6.1 Evaluation points

The vibration requirement of 26 nm is primarily prescribed for the magnets that are controlling the electrons and they are placed on concrete foundations in the storage ring tunnel. Due to the stiffness of the magnet foundations the vibrations will basically be the same at the bottom and the top positions of a magnet foundation. The evaluation points of the vibrations were picked at nodes along the floor where the magnet foundations are to be placed, as shown in Figure 6.1.

6.2 Harmonic loading

A parameter study was performed to investigate the behavior of the structure. The aim was to determine the vibration levels by varying the base parameters. This study was intended as a qualitative comparison of the vibration levels, i.e. the size of the loads and the magnitude of the results were not important, just the relative difference.

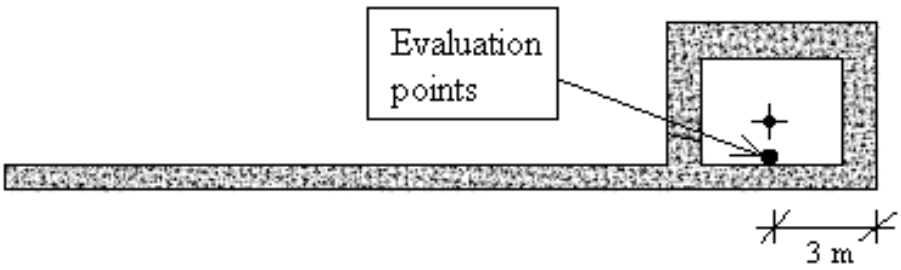

Figure 6.1: Modeled section with position of the evaluation points.

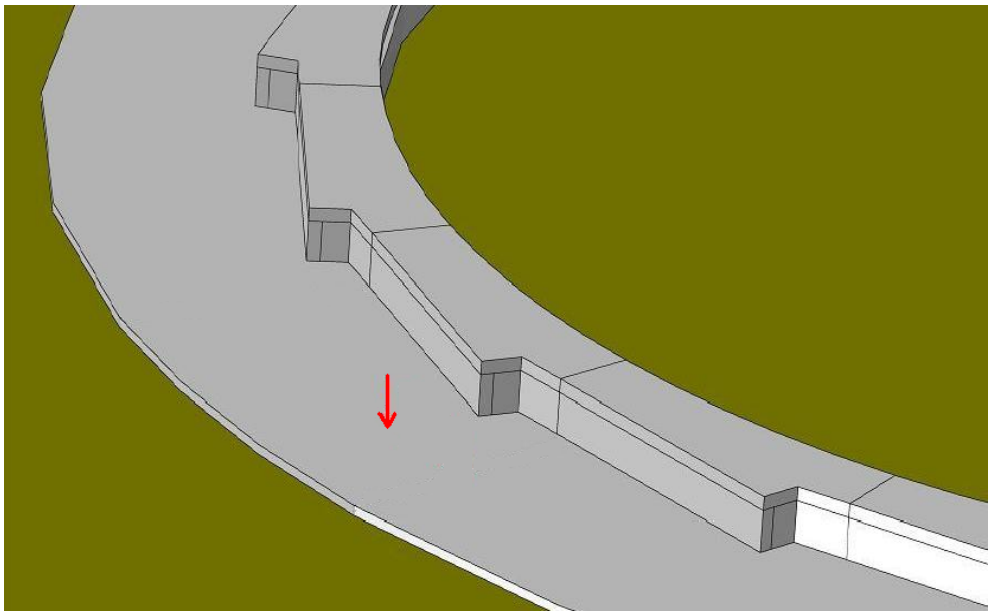

Figure 6.2: Position of the concentrated harmonic force.

The load was in the parameter study applied as a sinusoidal harmonic concentrated force with the magnitude of 1 kN. The load was positioned on the floor and 10 m from the outer boundary, as shown in Figure 6.2. The frequency of the load was varied from 0 to 40 Hz in steps of 1 Hz. All the resulting displacement versus frequency plots are shown in the Appendix.

Due to the harmonic loading, the analyses were performed in steady-state dynamics.

The results are presented in figures as plots of the maximum vertical displacement amplitude versus the various choice of parameters. The maximum vertical displacement amplitude of each case was sampled at the magnet foundation irrespective of which frequency it occurred at in the frequency range.

6.2.1 Young's modulus of concrete

A study was made to investigate the influence of various values of Young's modulus of concrete. Four analyses were made with different Young's modulus in the range 35-60 GPa. The range is set to cover values of realistic Young's modulus. A Young's modulus of 47 GPa is the highest value for classified concrete in Sweden, with the dynamic addition taken into account. This concrete type is called C 60/75.

As shown in the Appendix the displacements obtained by varying the values of Young's modulus of concrete essentially have the same frequency response. As shown in Figure 6.3 the displacement amplitudes only have a slight dependence on the

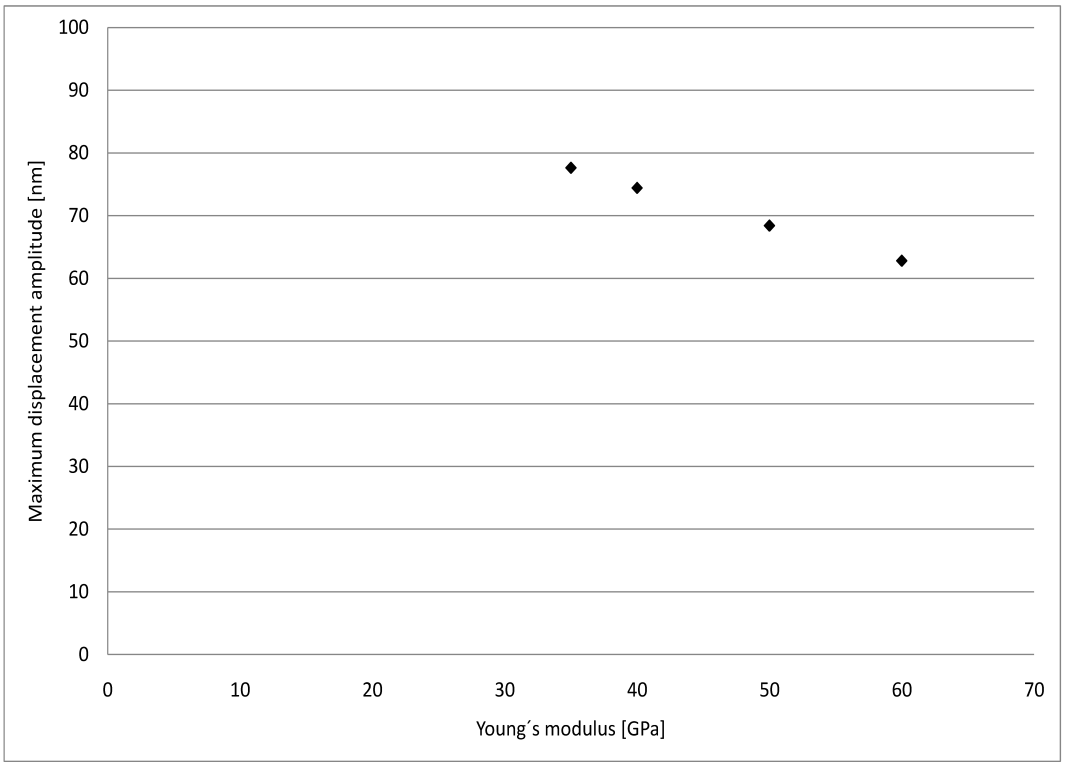

Figure 6.3: Maximum displacement amplitude for various Young's modulus of concrete.

Young's modulus. It could be of interest to use a high classified concrete type since high classified concrete have more benefits as well, for example the hardening time. It can be concluded that it would not make a significant difference to use a high classified concrete only to reduce the vibration levels.

6.2.2 Damping ratios

This study was made to investigate the influence of various damping ratios of the concrete and the soil on the vibration levels.

Four analyses were made for the concrete with damping ratios between 1 and 6 %, according to Figure 6.4. As shown in the Appendix the displacements obtained by varying the values of damping ratios of concrete essentially have the same frequency response. As shown in Figure 6.4 the damping ratio for concrete does not have a significant influence on the displacement amplitudes.

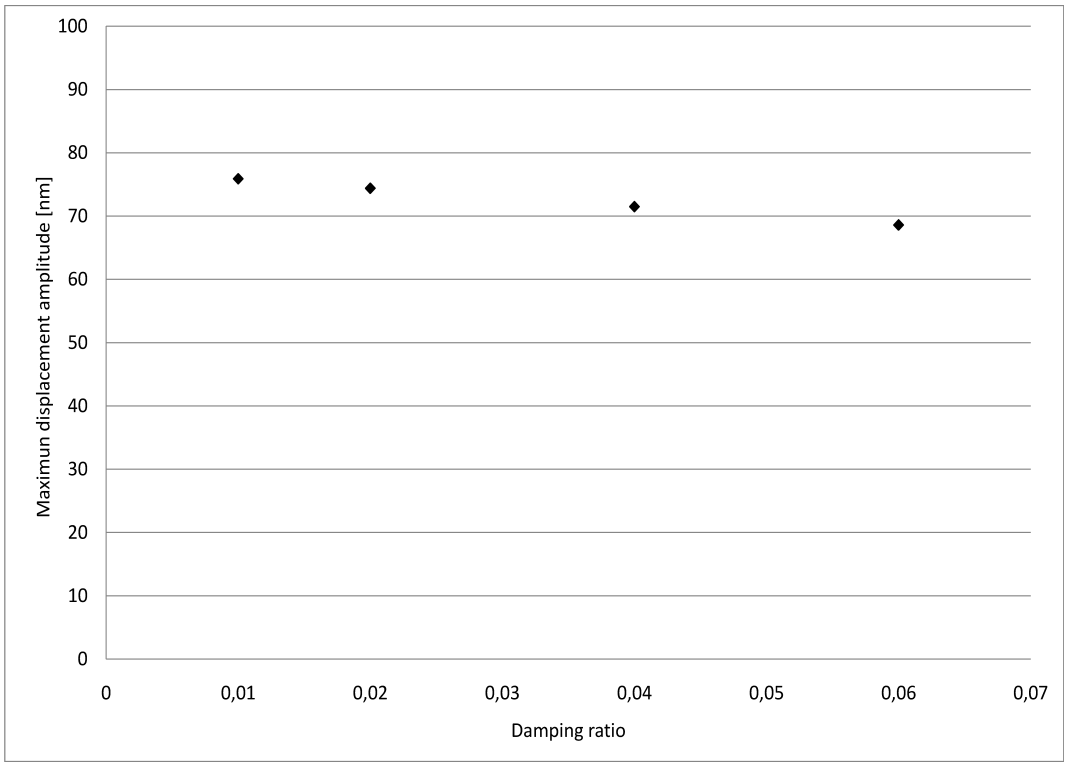

Figure 6.4: Maximum displacement amplitude for various damping ratios of concrete.

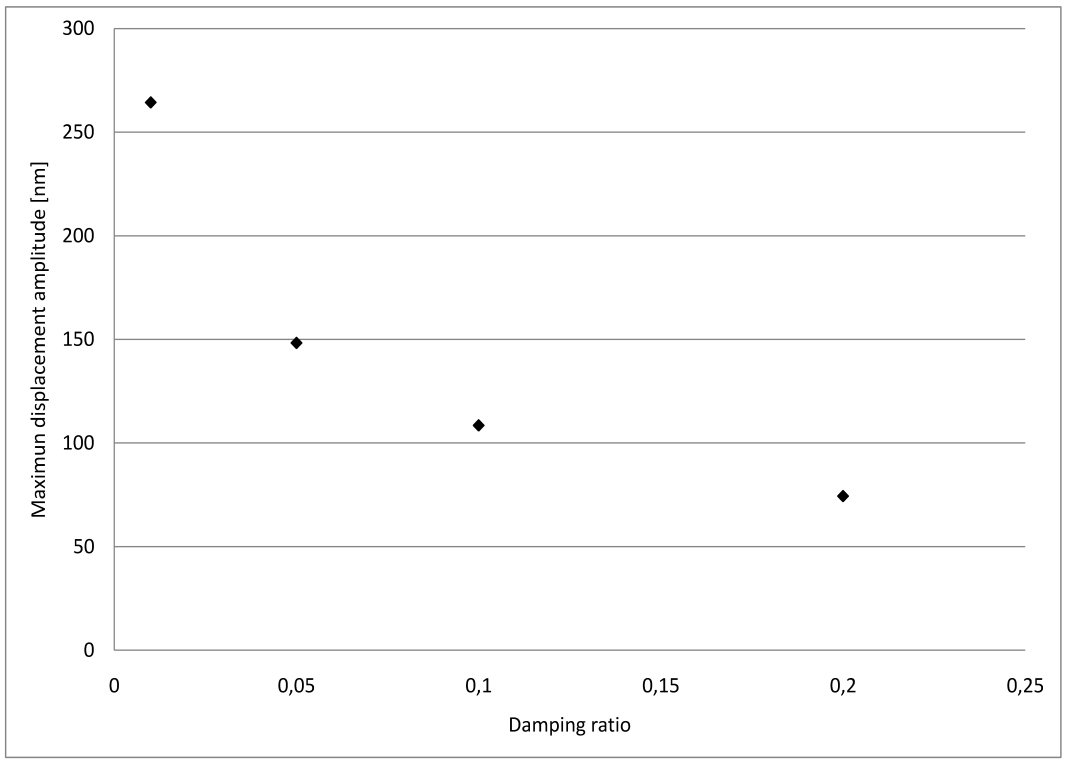

Figure 6.5: Maximum displacement amplitude for various damping ratios of soil.

Four analyses were made for the soil with damping ratios between 1 and 20 %, according to Figure 6.5. The damping ratio for the soil is computed for a larger span than for the concrete. This is done because of the uncertainness of the damping ratio of the soil. As shown in the Appendix the displacements obtained by varying the values of damping ratios of concrete essentially have the same frequency response. The damping ratio for the soil has a significant influence on the displacement amplitudes. This parameter is very uncertain as well, making it a very important parameter to determine through field measurements at site.

6.2.3 Thickness of the concrete floor

Several of the indoor loads directly affect the floor, such as, impact, walking and forklifts. Because of the large floor area a decrease of the thickness of the floor would significantly save time and money in the building phase due to the reduction of concrete and shortening of the casting process. Thus, the thickness of the floor has been varied from 500 to 2500 mm to determine the influence of thickness on the vibration levels.

The displacement versus the frequency for the evaluation point that generated the highest amplitude, considering 5-40 Hz, for each thickness of a floor thickness of 500 mm, 700 mm, 1000 mm, 1400 mm, 2000 mm and 2500 mm are shown in Figure 6.6. It is shown that a thicker floor generally lowers the vibration amplitudes. But for frequencies below 2 Hz the amplitudes have a tendency to increase with a thicker floor. A reason for this may be that a thicker floor increases the mass more than the stiffness and therefore lowers the natural frequency for the soil-structure system.

In Figure 6.7 it is shown that a thicker floor may cause higher amplitudes when considering all frequencies in the range of 0-40 Hz. This is because the floor is getting stiffer and therefore a different deflection shape occurs. This is only valid when there is a distance between the load position and the evaluation point. In Figure 6.8 it is shown that the breaking point for the benefit of increasing the thickness of the floor is reached at 2000 mm when considering 5-40 Hz regarding the vibration levels in the storage ring tunnel.

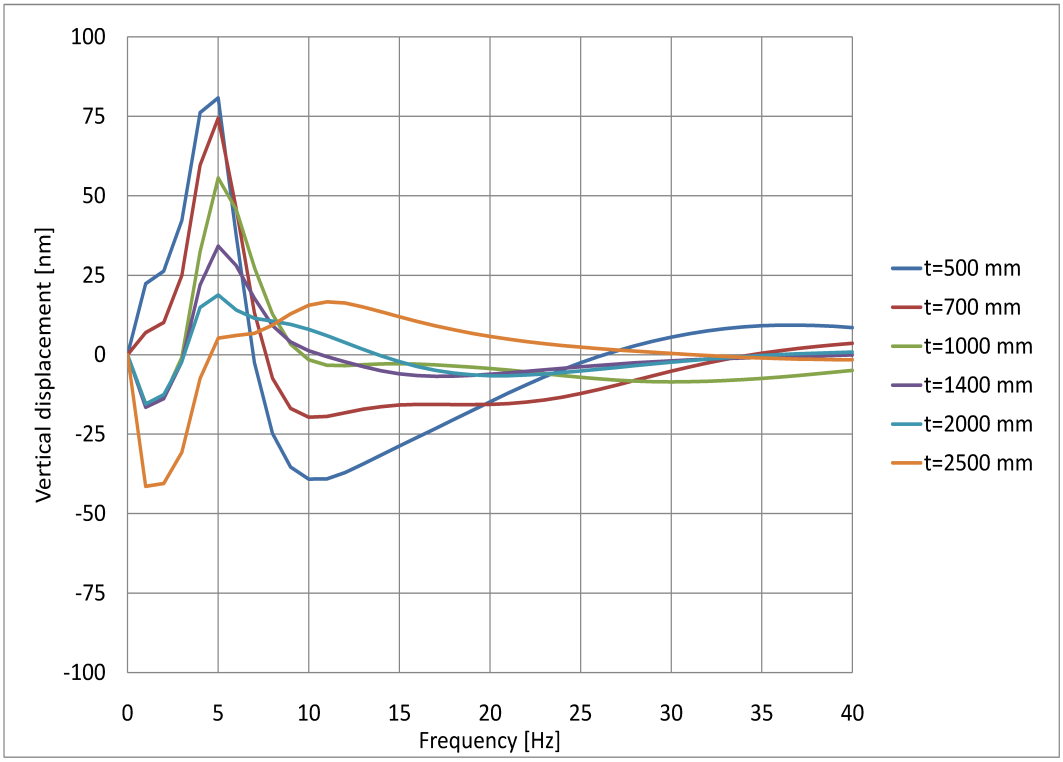

Figure 6.6: Displacement versus frequency for the evaluation point that generated the highest amplitude for each thickness of the concrete floor, only considering 5-40 Hz.

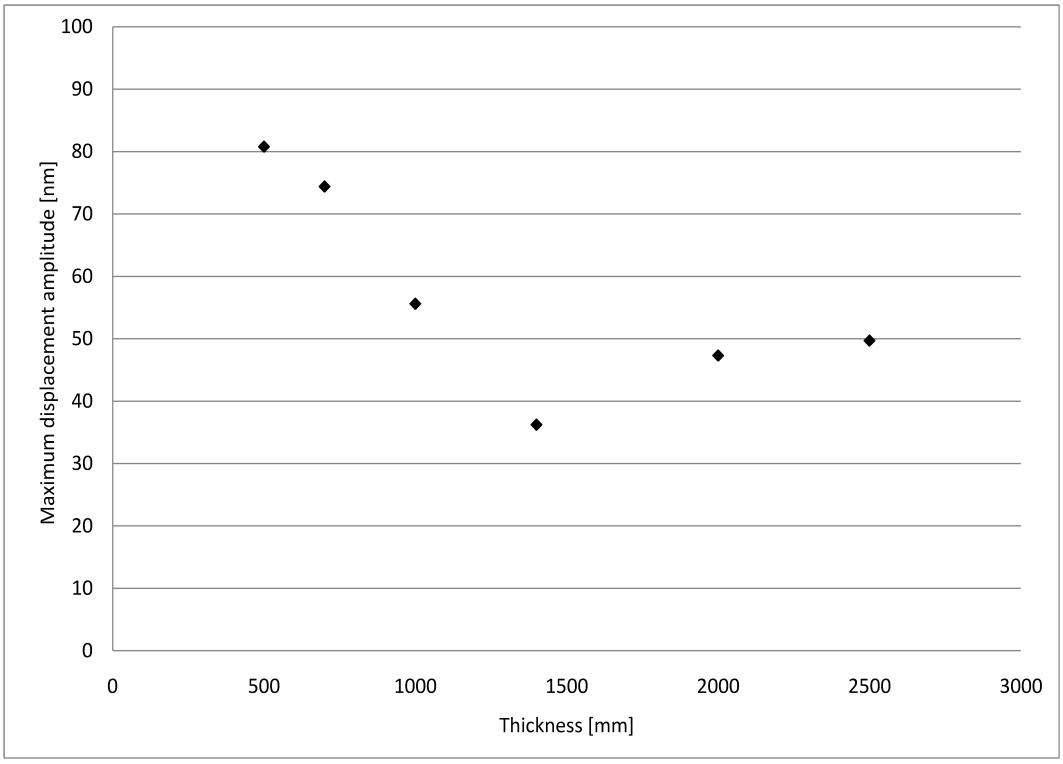

Figure 6.7: Maximum displacement amplitude for various thickness of the concrete floor.

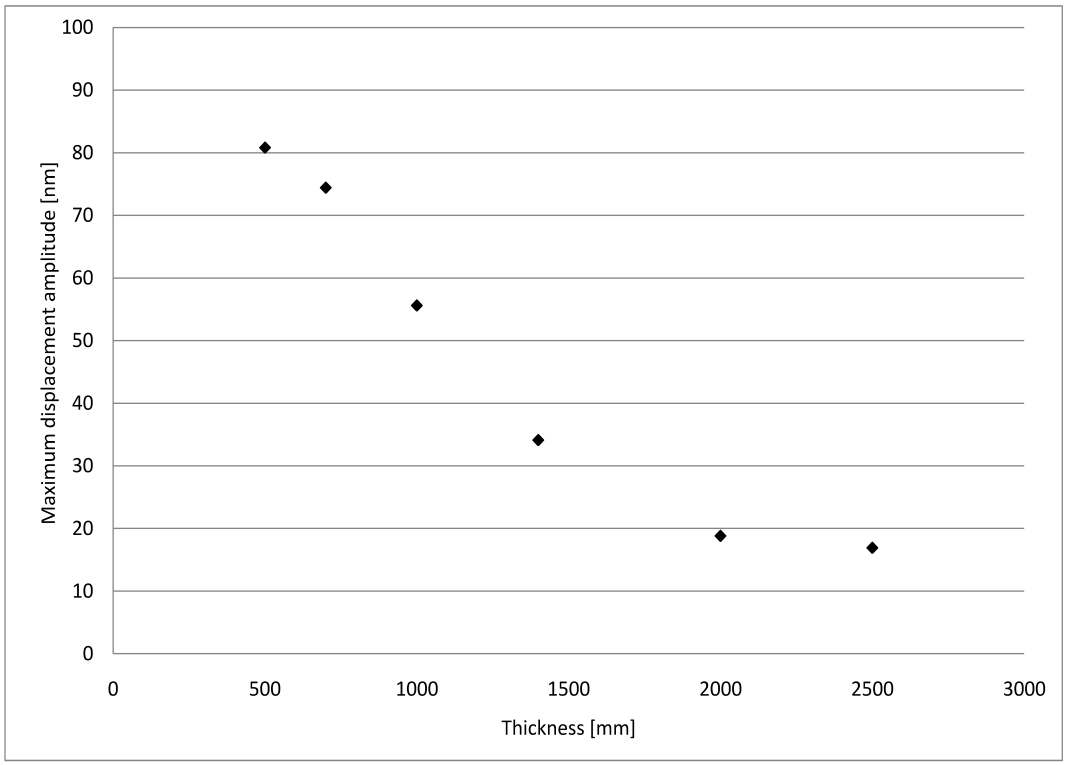

Figure 6.8: Maximum displacement amplitude for various thickness of the concrete floor, only considering 5-40 Hz.

6.2.4 Pillars

A study was made to investigate the influence of including pillars in the foundation of the floor on the vibration levels. Instead of modeling each pillar as discrete objects a smeared approach, according to Eq. 6.1, was made. This results in that the stiffness of the soil increases.

A volume-weighted Young's modulus was determined by

$$E_{new} = VE_{pillar} + (1 - V)E_{soil} \tag{6.1}$$

where V is the volume fraction of pillars in the soil.

The damping ratio and the density were not changed for the smeared model. The pillars were assumed to have a circular cross-section with a diameter of 0.4 m and being placed in a square pattern in the soil. The stiffness of all three soil layers were increased according to Eq.(6.1). This smeared approach will give approximate results but the general influence of the pillars is still shown.

Three analyses where made with an approximate distance between the pillars of 10 m, 5 m and 2 m, which correspond to a total number of pillars of 150, 600 and

3500 pillars.

In Figure 6.9 it is shown that increasing the number of pillars, the amplitude peaks decrease and occur at higher frequencies.

In Figure 6.10 it is shown that the displacements depend significant on the number of pillars in the soil, i.e. the stiffness of the soil. It was concluded from the approximate smeared approach that to get half the displacement amplitude around 150 pillars are needed. It can be concluded that pillars have a great influence on reducing the vibration levels.

A study was made to compare a thinner floor with pillars with a thicker floor with no pillars. The varying thickness of the floor is plotted for three different amount of pillars in Figure 6.11.

In Figure 6.11 it is shown that, for example, a 500 mm thick floor with 150 pillars has lower displacement amplitudes than 1400 mm floor with no pillars in the foundation of the floor. Moreover it also shows that for a large number of pillars in the foundation the thickness of the floor has less importance on the vibration levels.

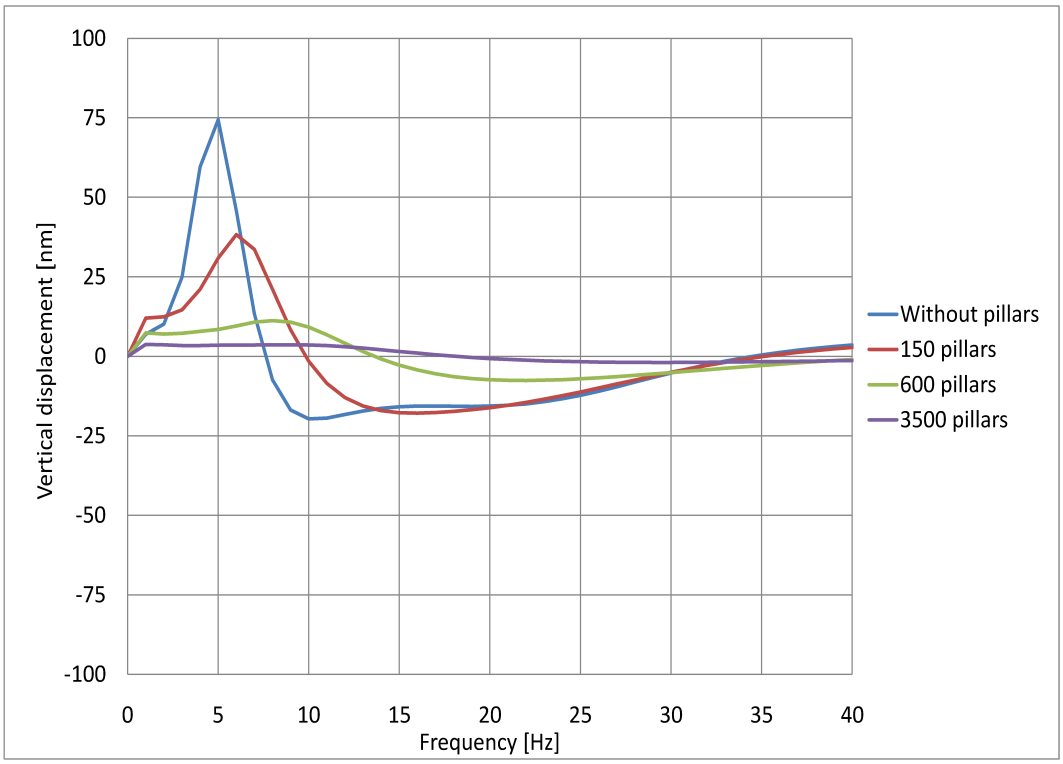

Figure 6.9: Displacement versus frequency for the evaluation point that generated the highest peak for each amount of pillars.

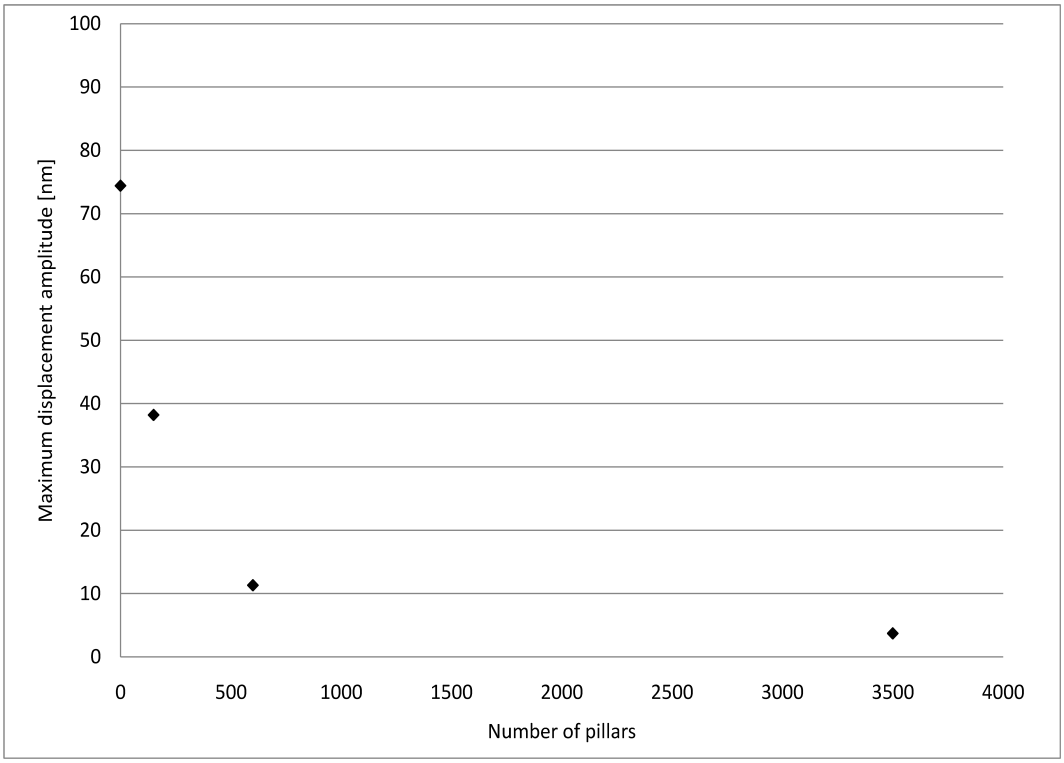

Figure 6.10: Maximum displacement amplitude for various number of pillars.

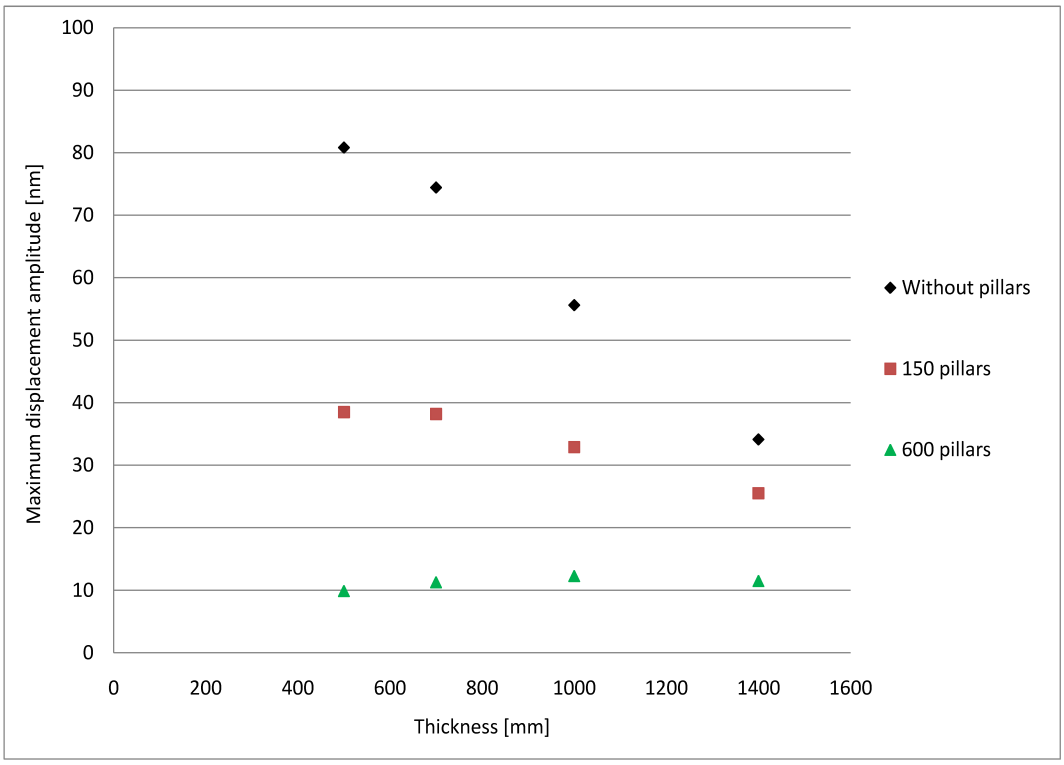

Figure 6.11: Maximum displacement amplitude for various number of pillars and thickness of the concrete floor.

6.2.5 Divided floor

A study was made to investigate the influence of a divided floor with a 4 m wide walking/driving way at the outer boundary that is separated from the laboratory floor. In Figure 6.13 the divided floor is shown. Three analyses were made with various loading positions for both the original floor structure as well as the divided floor structure, according to Figure 6.12 and Figure 6.13.

Table 6.1: *Load positions.*

Load position	Distance from the outer boundary
1	1 m
2	2 m
3	3 m

As shown in the Appendix the displacements obtained by investigate the influence of a divided floor essentially have the same frequency response as for the original floor geometry. In Figure 6.14 it is shown that the solution that will generate the lowest displacement amplitudes depends on the load position. Since the floor is divided, the vibration waves are propagating through the soil. The reason that the displacement amplitudes can be higher in the divided floor is that the floor is getting lower bending stiffness due to the reduced floor area.

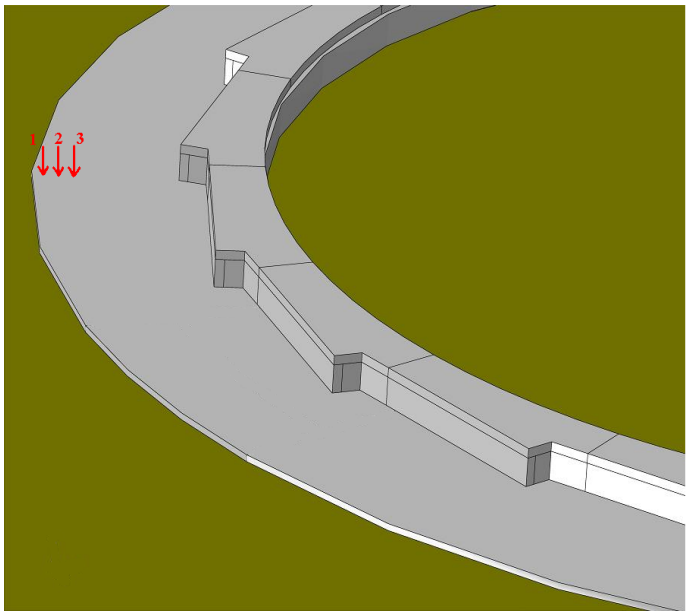

Figure 6.12: Load positions for the original floor.

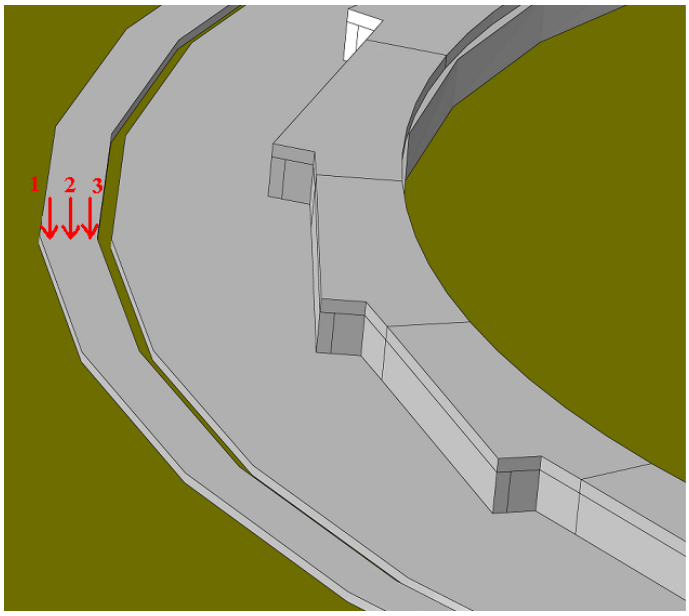

Figure 6.13: Load positions for the divided floor.

The study of using a divided floor was also combined with that of having 600 pillars. In Figure 6.15 it is shown that the solution that would generate the lowest displacement amplitudes is depending on the load position. This is the same behavior as shown in Figure 6.14.

It was concluded that it is not a benefit to have a divided floor since walking and other human activities not have a fixed load position.

6.2.6 General conclusion

It was concluded that the main influence on the vibration levels at the magnet foundations of the storage ring are the properties of the soil. Both the damping ratio of the soil and the influence of pillars have a significant influence of the vertical displacement of the magnet foundations.

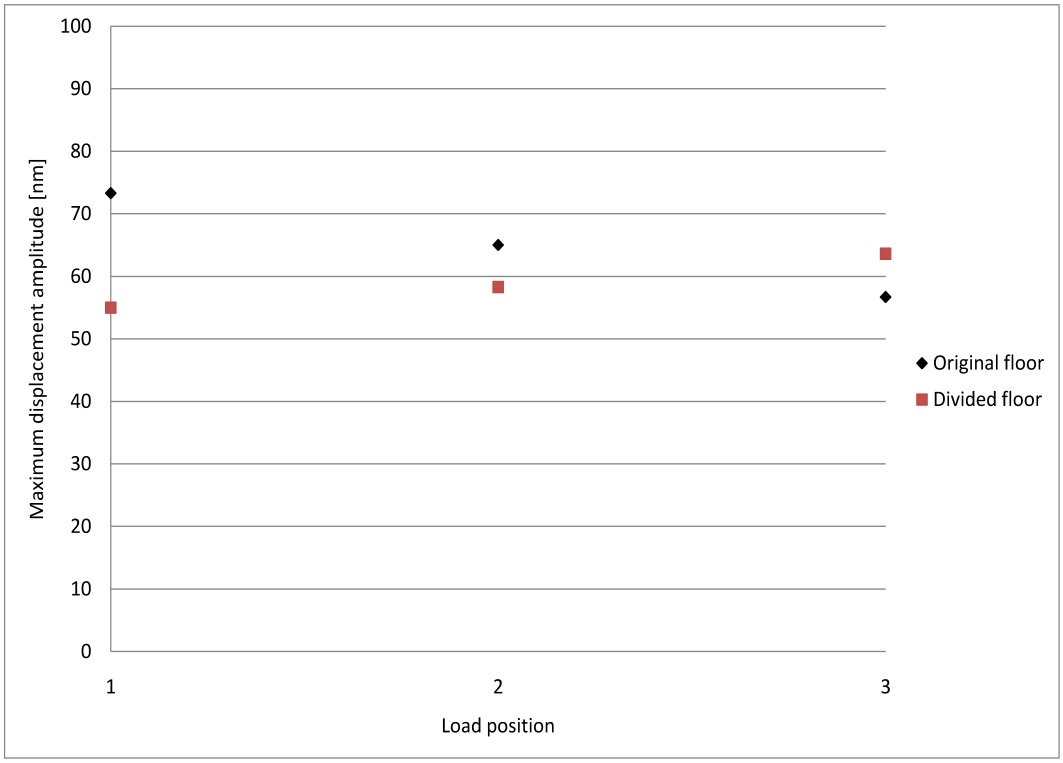

Figure 6.14: Maximum displacement amplitude with the influence of a divided floor.

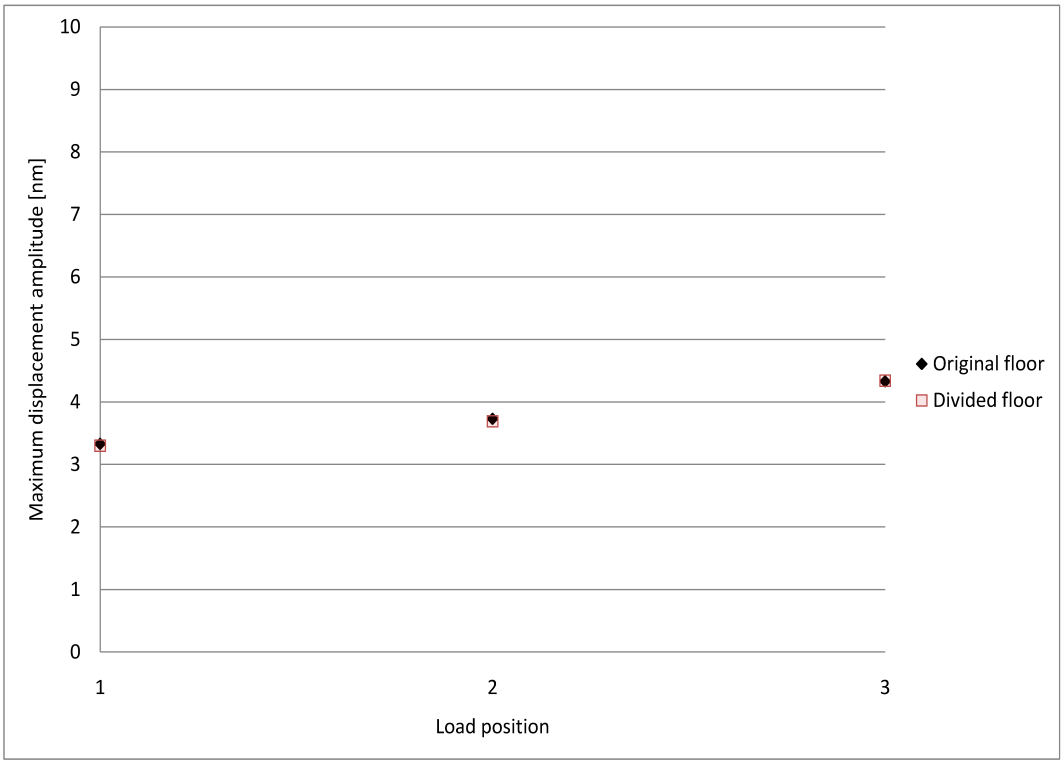

Figure 6.15: Maximum displacement amplitude with the influence of a divided floor with pillars.

6.3 Transient loading

6.3.1 Human walking

Human walking may be described as a dynamic load and should be considered in building design to meet the serviceability condition. In this case it is the displacement of the magnets that determines the requirement. Vibrations induced by human walking are depending on the "crowd effect" i.e. how many persons there are walking. In this study a simplified case of the walking load was applied by only consider one person walking. The walking load was modeled as a transient moving load with time varying amplitudes. The amplitude of a gait cycle of two footsteps is shown in Figure 6.16. The time period is 0.55 s which results in a gait cycle frequency of 1.8 Hz.

Normally, the loading should be applied on two discrete circles, one representing the heel and one the forefoot, [7]. However, since the foot size is so small compared to the floor extension, the foot load was modeled as a concentrated force instead of two discrete circles.

The walking pattern was constructed from a study of the walking pattern for 150 men. Figure 6.16 and Table 6.2 shows detailed gait parameters from the measurements in [8].

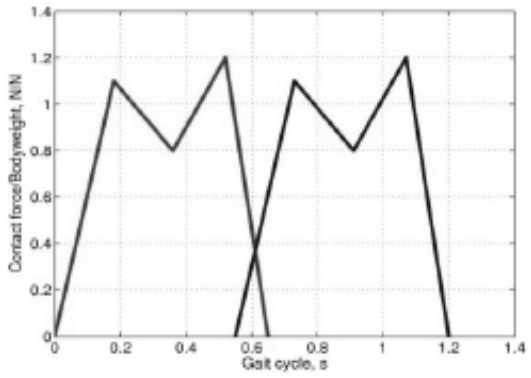

(a) Gait cycle, [7].

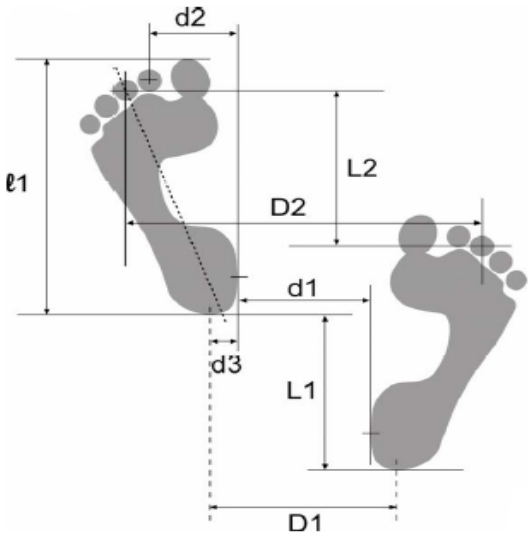

(b) Detailed gait parameters, [8].

Figure 6.16: Gait cycle and gait parameters.

Only the parameters L_1 and L_2 in Table 6.2 was considered here since the loading was applied on a straight line, because of the floor extension. The lengthwise distance was set to 65 cm according to Table 6.2.

Table 6.2: *Detailed gait parameters, [8].*

Parameter	Value [cm]
l_1	26.5
L_1	65
L_2	65
d_1	5
d_2	5
d_3	2.2
D_1	10
D_2	19

6.3.2 Walking load

To simulate the walking load as realistic as possible, it was applied as a transient moving load. Analyses were made for two load patterns on the concrete floor corresponding to tangential and radial walking patterns. The duration of the analyses of the walking patterns was 7 s.

The tangential walking pattern was positioned 10 m from the outer boundary of the concrete floor as shown in Figure 6.17. The radial walking pattern started at the outer boundary of the storage ring tunnel and was directed towards the outer boundary of the floor, as shown in Figure 6.18.

6.3.3 Results

The time dependent vertical displacement amplitude for the nearby evaluation points in the storage ring tunnel are presented for the tangential walking pattern in Figure 6.19 and for the radial walking pattern in Figure 6.20.

From the results of the tangential walking pattern, as shown in Figure 6.19, it was found that the displacement amplitudes follow the load amplitudes but with a smoother response and a phase lag between the load and the response due to the damping in the structure. As expected, the peak values of the displacement amplitudes are constant due to the constant distance to the evaluation points. The evaluation point where the highest peak was located altered as the load was moving.

From the results of the radial walking pattern, as shown in Figure 6.20, it was found

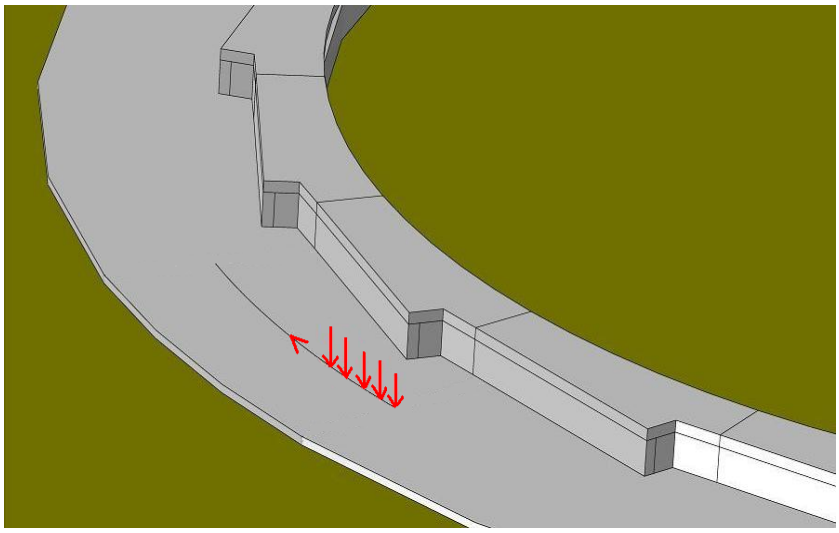

Figure 6.17: Position of the tangential walking pattern.

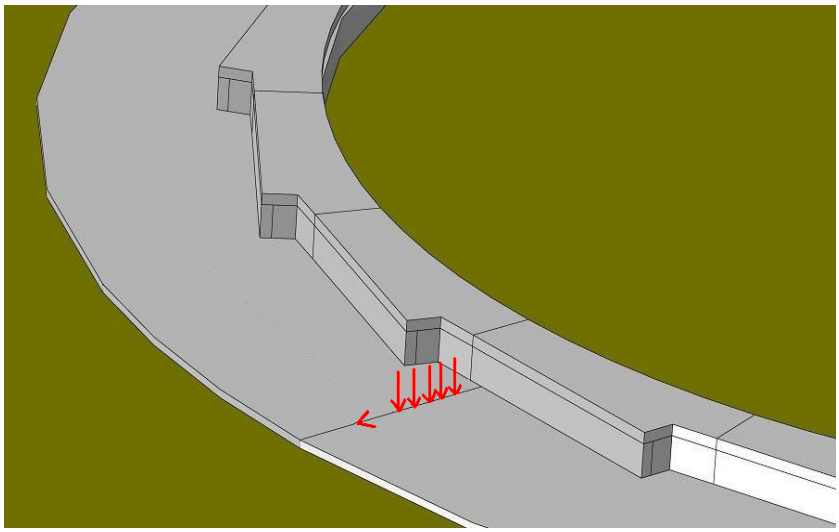

Figure 6.18: Position of the radial walking pattern.

that the displacement amplitudes follow the load amplitudes but with a smoother response and a phase lag between the load and the response due to the damping in the structure. The difference of the radial from the tangential walking pattern was that the load was moving away from the evaluation points. As can be seen in Figure 6.20, the displacement is decreasing with time due to the load was moving away from the evaluation points.

In order to relate the results to the requirements the RMS-value was calculated. The RMS-value of the total vertical displacement was calculated for the one-second period of the simulation time that resulted in the highest RMS-value. This calculation was done with a code in the computer program *Matlab* that makes a sweep in time and present the value of the second with the highest RMS-value of the total displacement. The RMS-value of the total displacement includes both the static and the dynamic part of the displacement. The static part may require a weaker requirement than the dynamic part, therefore the RMS-value for the dynamic part was also calculated. The RMS-value was calculated for all frequencies even those below 5 Hz where weaker requirement of 260 nm instead of 26 nm is required. Table 6.3 shows the different RMS-values for the different walking patterns. Table 6.4 shows the static deflection for the different walking patterns.

Table 6.3: *RMS-value of the vertical displacement.*

Walking pattern	Total	Dynamic
Tangential	12 nm	4 nm
Radial	105 nm	18 nm

Table 6.4: *Static deflection of the vertical displacement.*

Walking pattern	Deflection
Tangential	11 nm
Radial	103 nm

In Table 6.3 and Table 6.4 it is shown that the static part is much bigger than the dynamic part. Even though the static part may be less important, the dynamic part of the radial walking was close to exceeded the requirement of 26 nm. The resulting RMS-value for the total displacement for the radial walking exceeded the requirement of 26 nm. It was concluded that walking loads, especially from groups of people, must be considered in the design process.

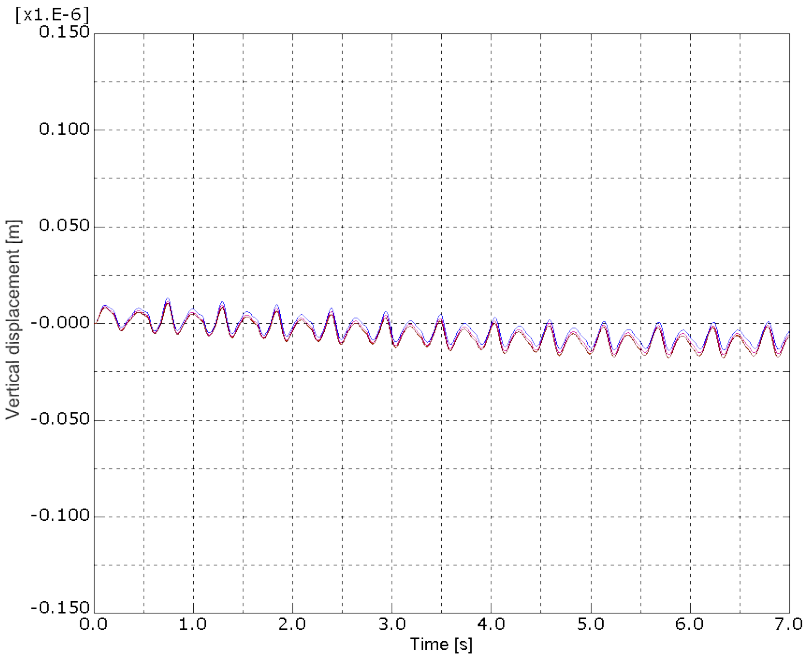

Figure 6.19: Plot in time domain for tangential walking pattern.

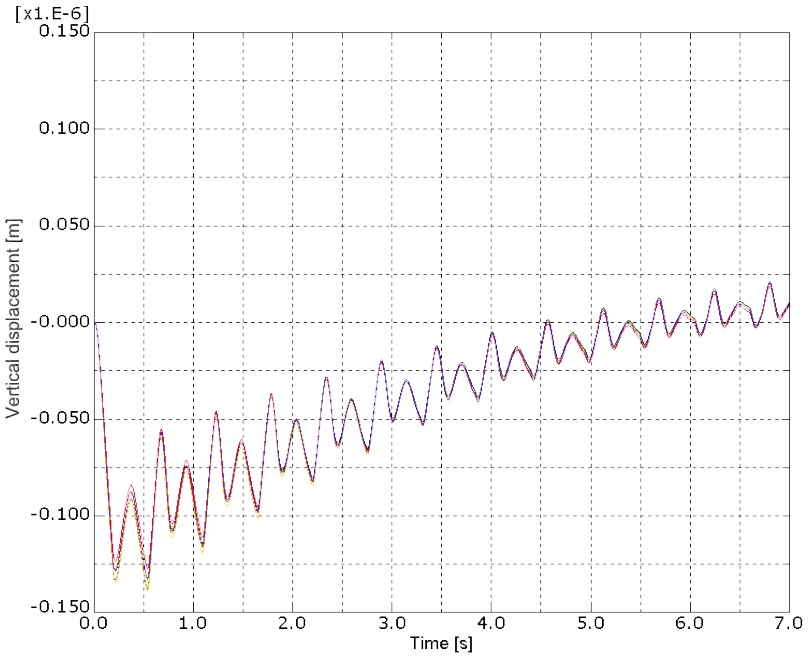

Figure 6.20: Plot in time domain for radial walking pattern.

7

Discussion and Suggestions for Further Work

It was discovered from the parameter study that the material parameters of the soil greatly influences the vibration levels of the floor. Since there is a lack of knowledge regarding the material parameters for the soil there is a need for determining those. There are especially two parameters for the soil that control the soil and thus the structure; the Young's modulus and the damping ratio. The Young's modulus is given in the geotechnical report but it should not be used for detailed design. For the bedrock there is no information about material parameters. The material parameters are needed to get a reliable output that can be compared with the requirements.

The smeared approach that was used to determine the equivalent stiffness of the soil when considering the pillars was an approximation. How good the results from this approximation are depending on several things like the bending wave length and the position of the pillars. To get more reliable results discrete pillars would be introduced discrete pillars in the model.

In the parameter study, the harmonic load was only applied at one location. The loading position should be varied because the relation between the thickness of the floor and the displacement of the evaluation points depends of the distance between the load position and the evaluation point.

To ensure that the strict requirements are fulfilled, more realistic loads must be considered. Such loads are for instance working machines, traffic from inside the building such as forklifts and outside such as traffic from nearby roads. Also a group of people walking must be considered. A FFT should also be done for the displacements in the time domain to see the frequency content of the walking load. It may be shown in the frequency domain that some peaks are below 5 Hz and may therefore be excluded from the calculations of the RMS-value.

If the traffic load from the nearby highway are to be analysed the Linac and the storage ring must be considered in the same model since the Linac could work as a barrier for the vibrations from the traffic due to its position between the ring and the highway.

Besides from the opportunities given in the parameter study dampers can be used as a solution to reduce the vibration levels. For one example the influence of rubber mats could be investigated.

Bibliography

[1] Boverket (2004). *Boverkets handbok om betongkonstruktioner, BBK 04.* Boverket

[2] Ottosen N. S. and Petersson H. (1992). *Introduction to the finite element method.* Prentice Hall

[3] Anil K. Chopra (1995). *Dynamics of structures.* Prentice Hall

[4] Engström Björn (2004). *Beräkning av betongkonstruktioner.* Institutionen för konstruktion och mekanik, Chalmers tekniska högskola.

[5] Axelsson Kennet (2005). *Introduktion till GEOTEKNIKEN.* Instutitionen för Geovetenskaper, Uppsala Universitet.

[6] Sällfors Göran (2008). *Kurspärm GRUNDLÄGGNINGSTEKNIK.* Instutionen för Byggvetenskaper, Lunds Universitet.

[7] Bard Delphine, Persson Kent & Sandberg Göran (2008). *Human footsteps induced floor vibration.* Acoustics'08, Paris France, July 2008.

[8] Claesson Jimmy (2008). *Simulering av stomljud med hjälp av gångmönsterstatistik* Division of Engineering Acoustics, Lunds Tekniska Högskola, Report TVBA 5038.

[9] SIMULA (2008). *Abaqus manual 6.9*

[10] Heyden Susanne, Dahlblom Ola, Olsson Anders & Sandberg Göran. (2007). *Indroduktion till Strukturmekaniken* KFS i Lund AB

[11] MAX-lab, Lunds Universitet. (2009). *MAX-lab - MAX IV*

[12] SWECO AB. (2009). *Drawings MAX IV*

[13] Ohlrich M, Hugin C.T. (2003). *On the influence of boundary constraints and angled baffle arrangements on sound radiation from rectangular plates* Journal of Sound and Vibration 277, 2004.

[14] SWECO AB. (2009). *MAX IV, LUND. ÖVERSIKTLIG GEOTEKNISK UTREDNING (TPgeo).*

Appendix A

Plots of frequency sweeps

Plots of frequency sweeps for varying parameters according to the parameter study in Modelling Results.

Young's modulus of concrete

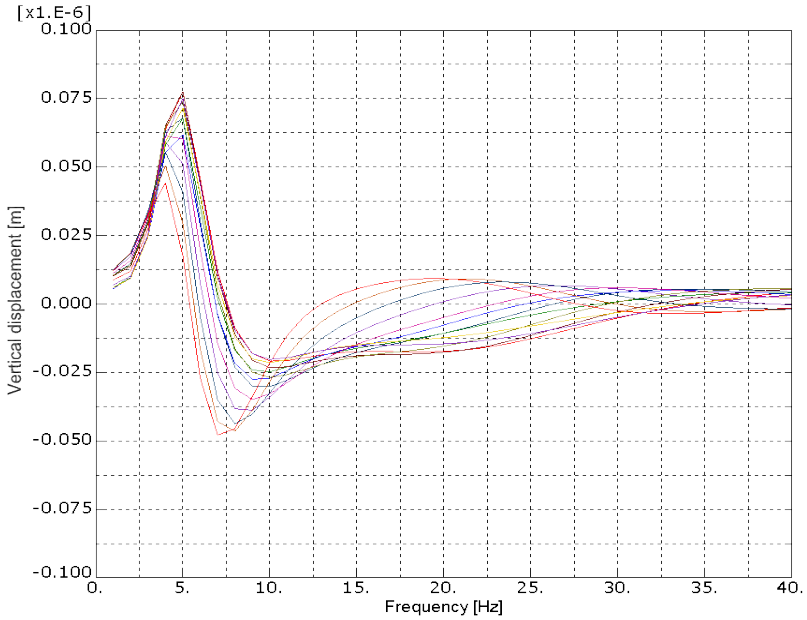

Figure A.1: Displacement vs frequency, Young's modulus of concrete is 35 GPa.

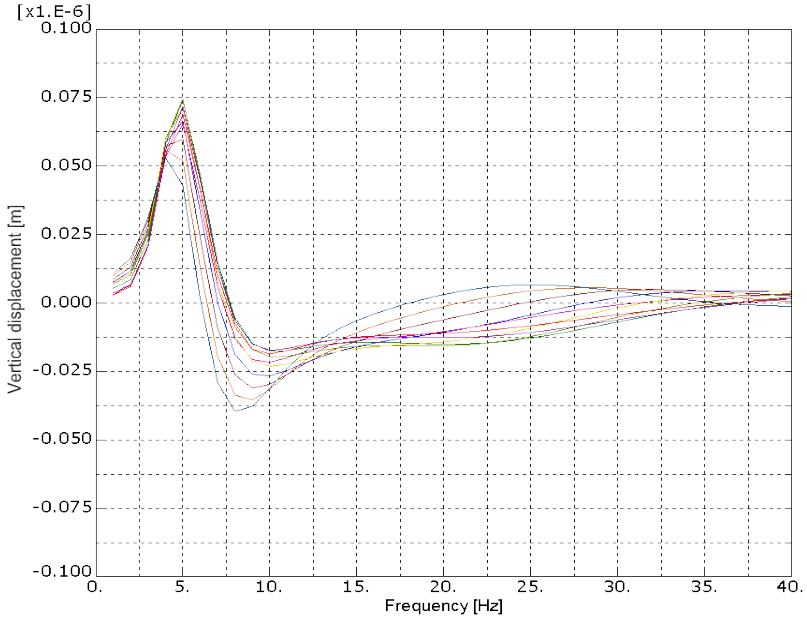

Figure A.2: Displacement vs frequency, Young's modulus of concrete is 40 GPa.

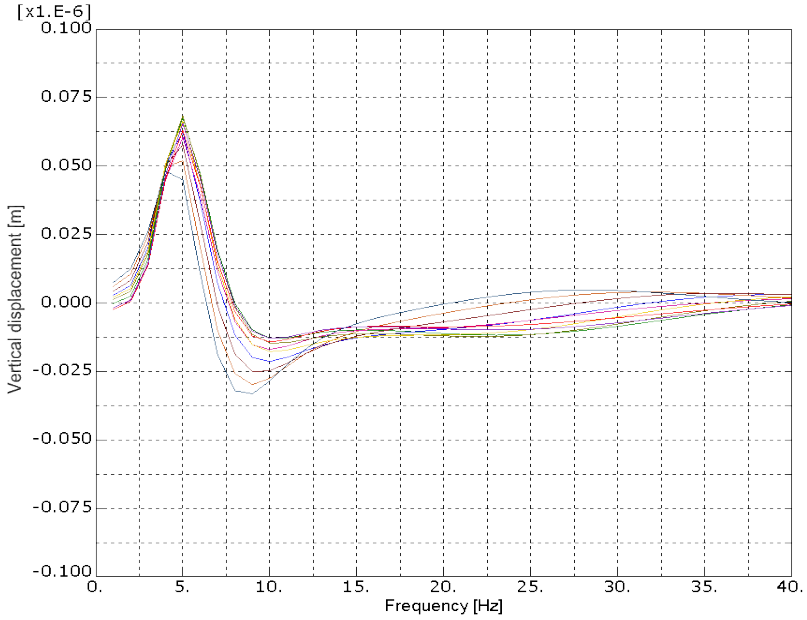

Figure A.3: Displacement vs frequency, Young's modulus of concrete is 50 GPa.

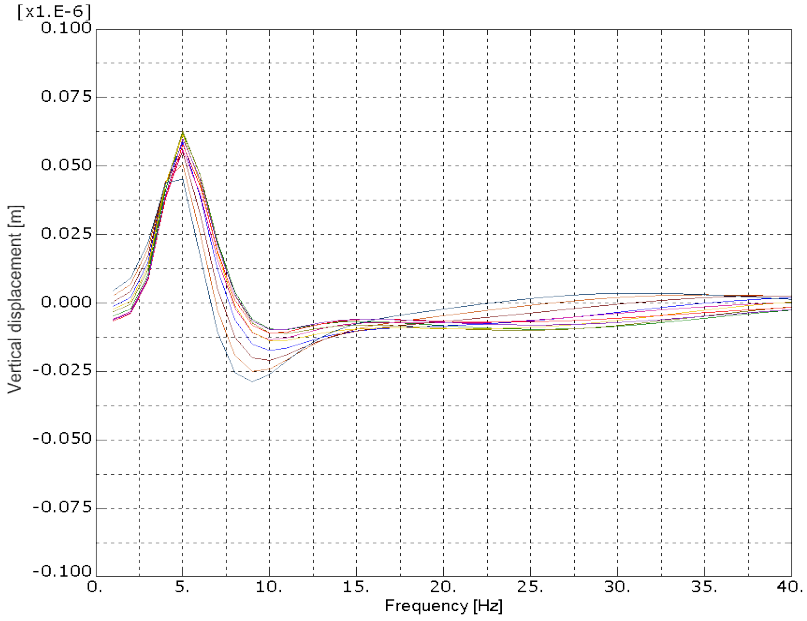

Figure A.4: Displacement vs frequency, Young's modulus of concrete is 60 GPa.

Damping ratio of concrete

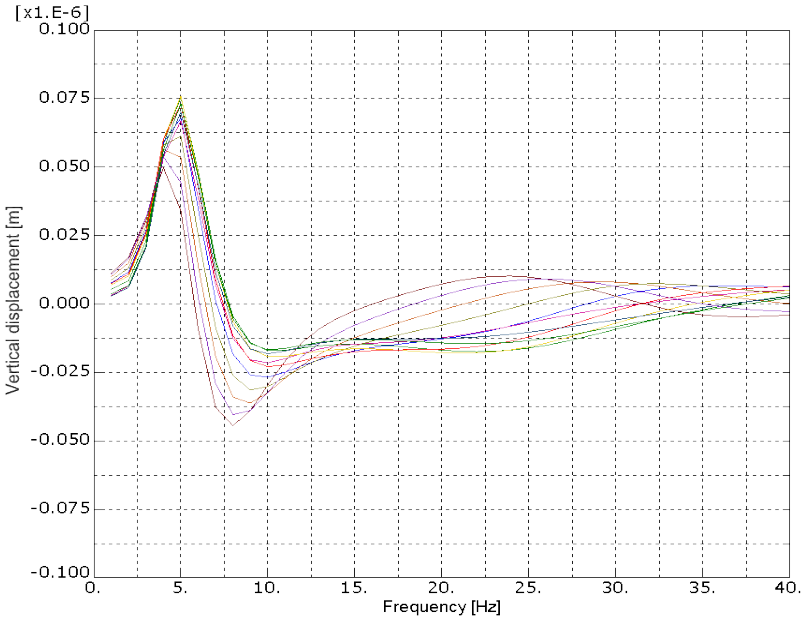

Figure A.5: Displacement vs frequency, damping ratio of concrete is 1 %.

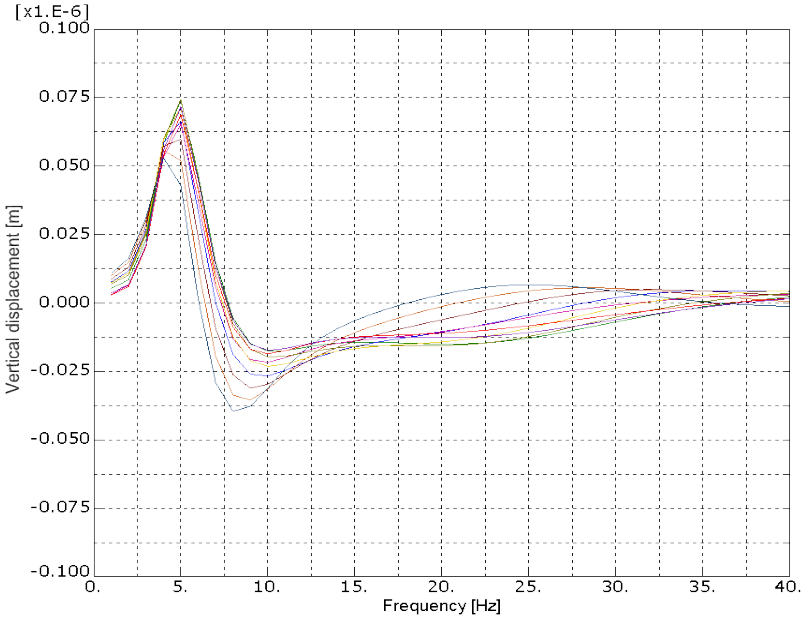

Figure A.6: Displacement vs frequency, damping ratio of concrete is 2 %.

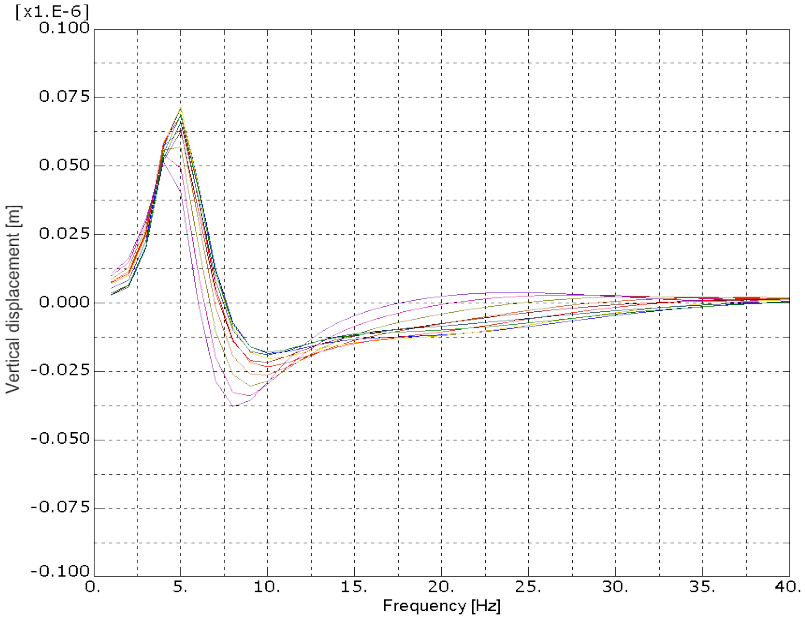

Figure A.7: Displacement vs frequency, damping ratio of concrete is 4 %.

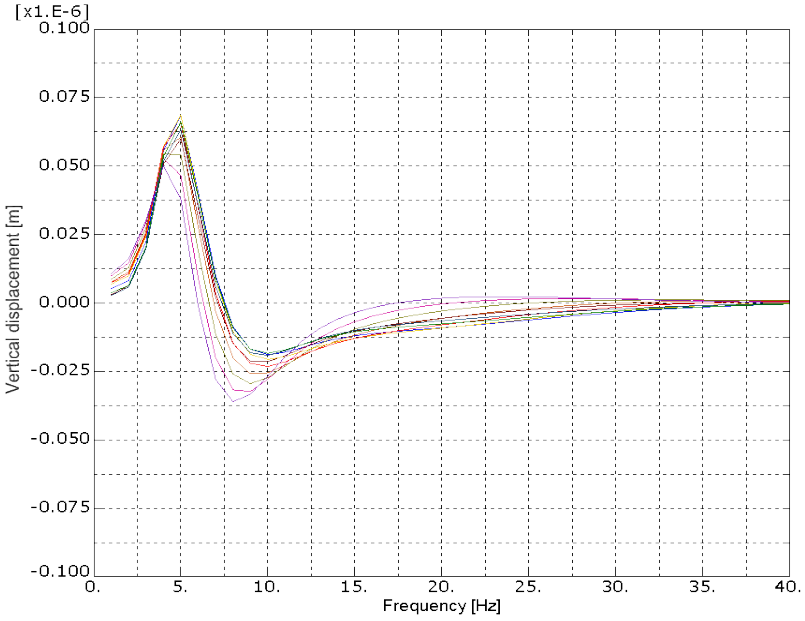

Figure A.8: Displacement vs frequency, damping ratio of concrete is 6 %.

Damping ratio of soil

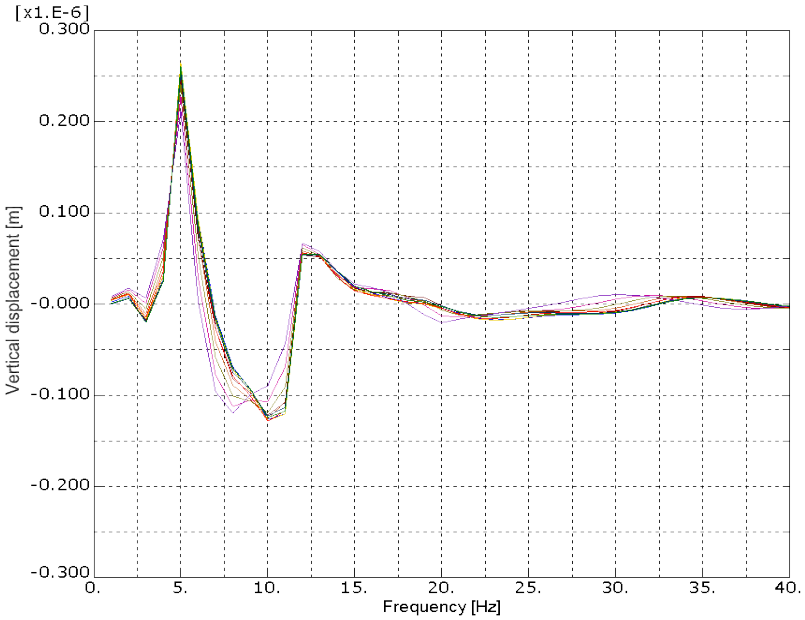

Figure A.9: Displacement vs frequency, damping ratio of soil is 1 %.

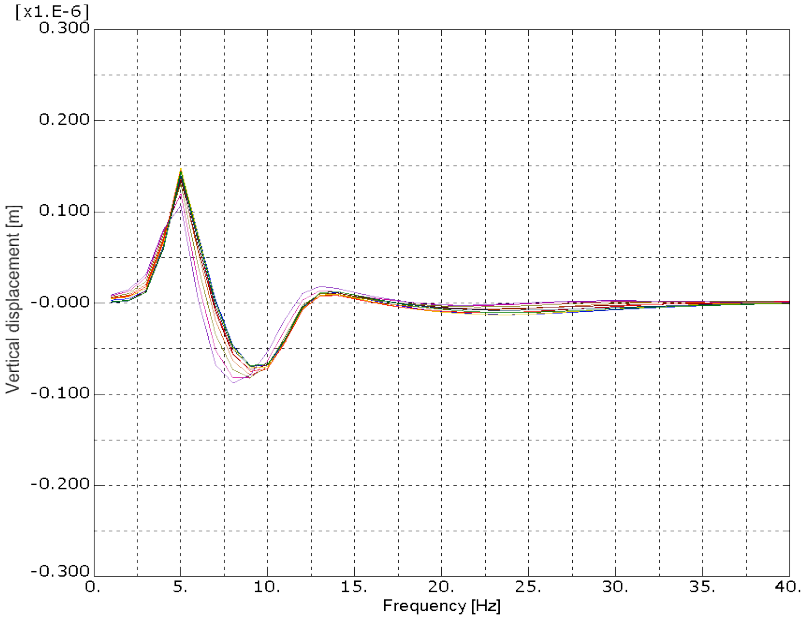

Figure A.10: Displacement vs frequency, damping ratio of soil is 5 %.

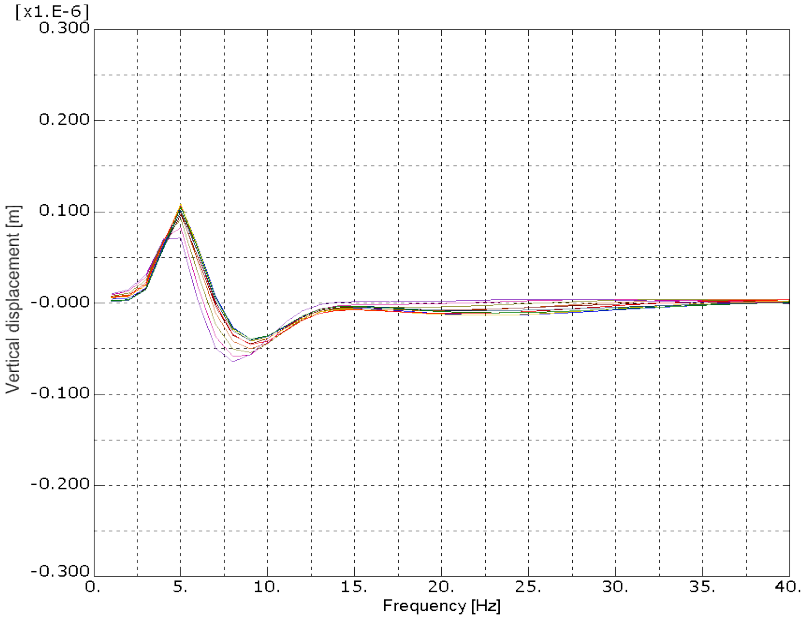

Figure A.11: Displacement vs frequency, damping ratio of soil is 10 %.

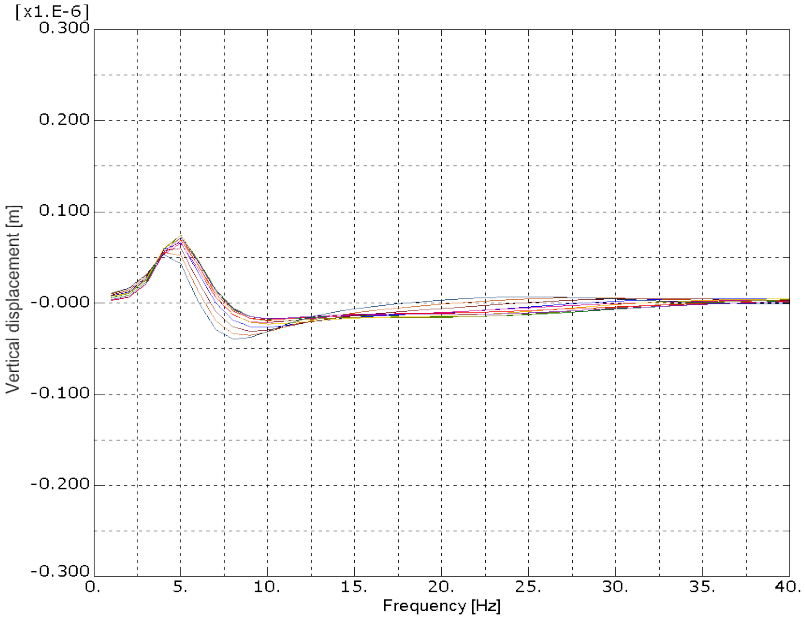

Figure A.12: Displacement vs frequency, damping ratio of soil is 20 %.

Thickness of the concrete floor

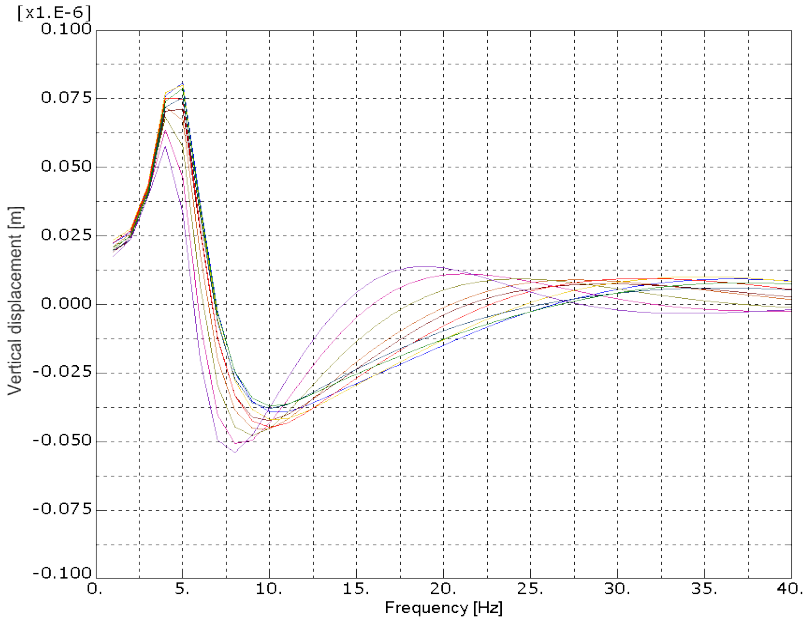

Figure A.13: Displacement vs frequency, floor thickness of 500 mm.

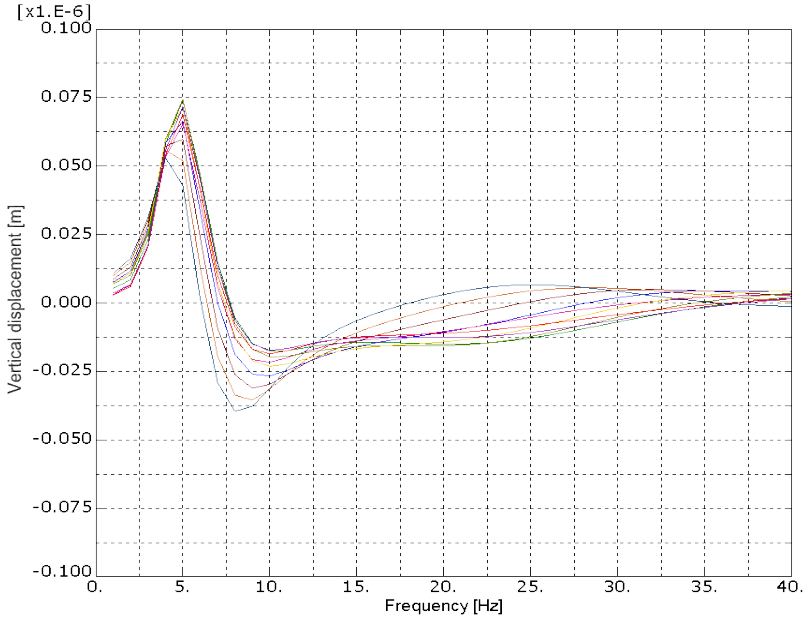

Figure A.14: Displacement vs frequency, floor thickness of 700 mm.

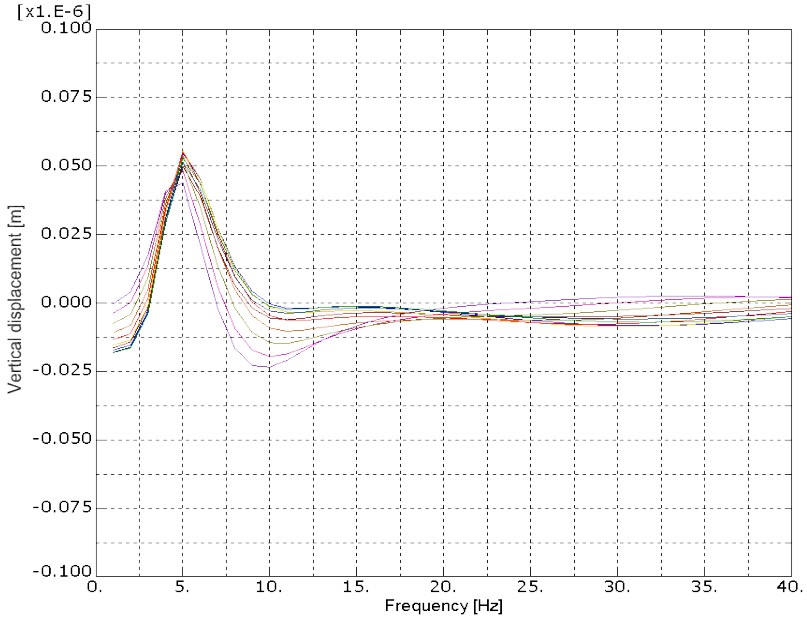

Figure A.15: Displacement vs frequency, floor thickness of 1000 mm.

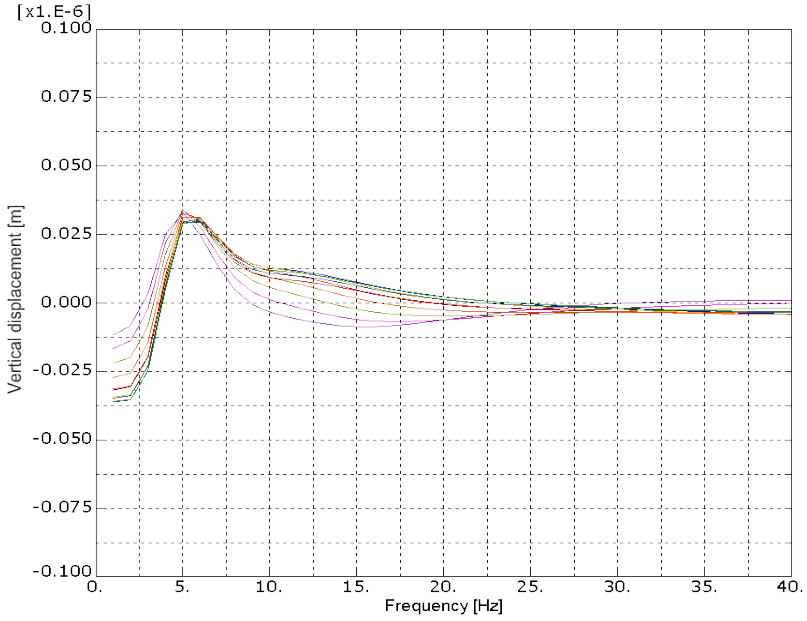

Figure A.16: Displacement vs frequency, floor thickness of 1400 mm.

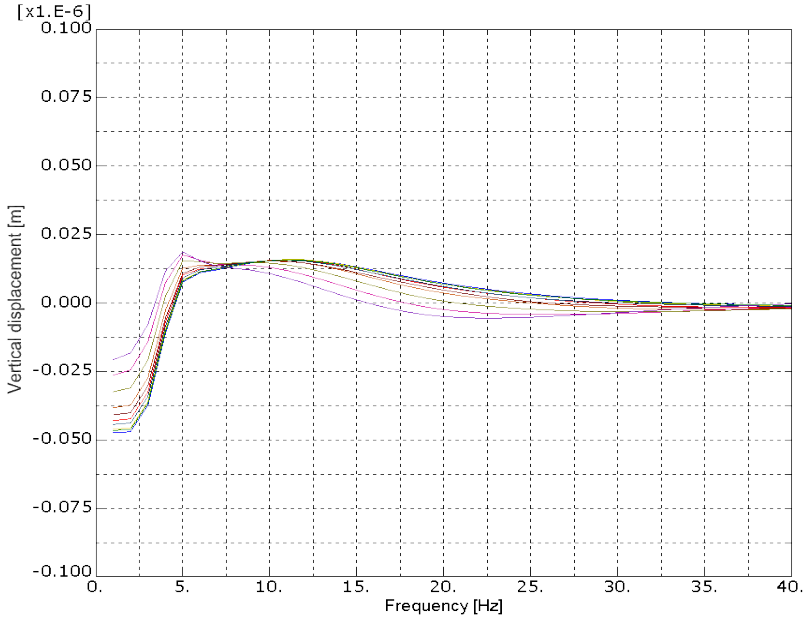

Figure A.17: Displacement vs frequency, floor thickness of 2000 mm.

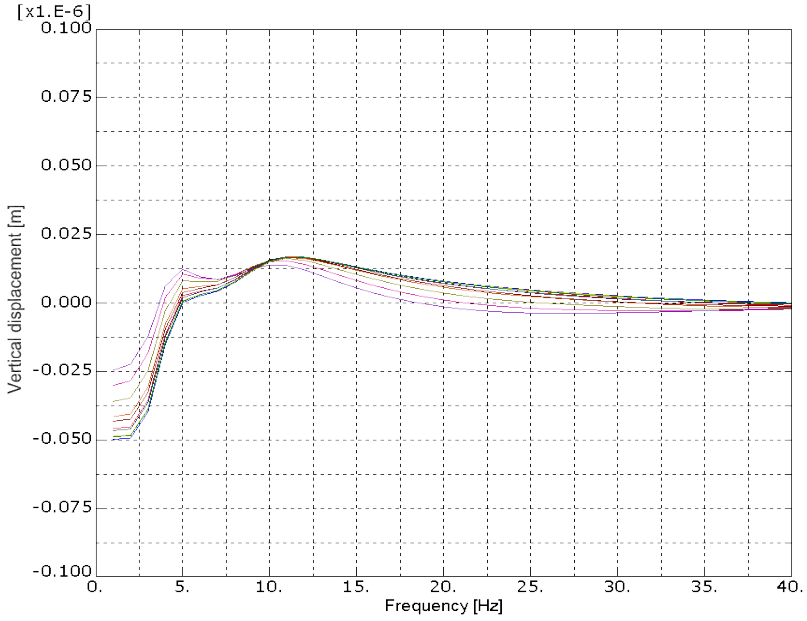

Figure A.18: Displacement vs frequency, floor thickness of 2500 mm.

Pillars

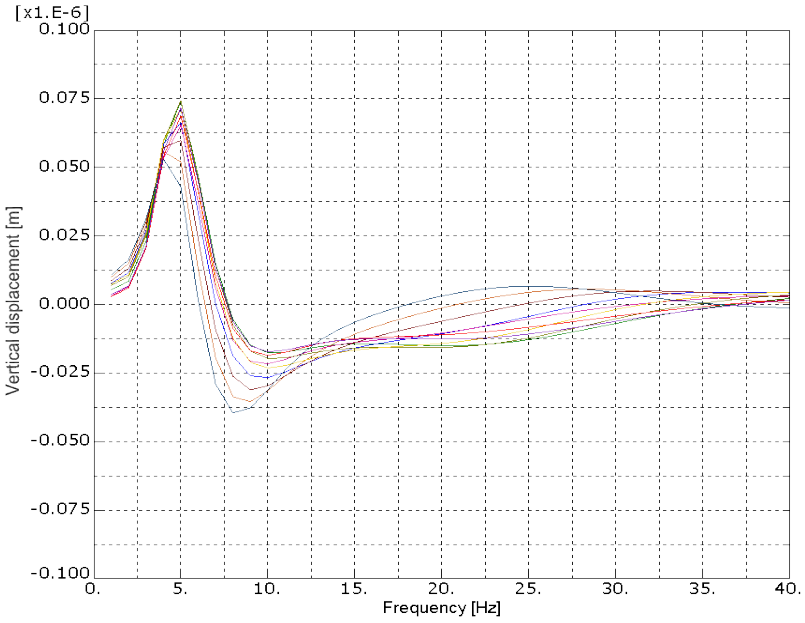

Figure A.19: Displacement vs frequency, without pillars.

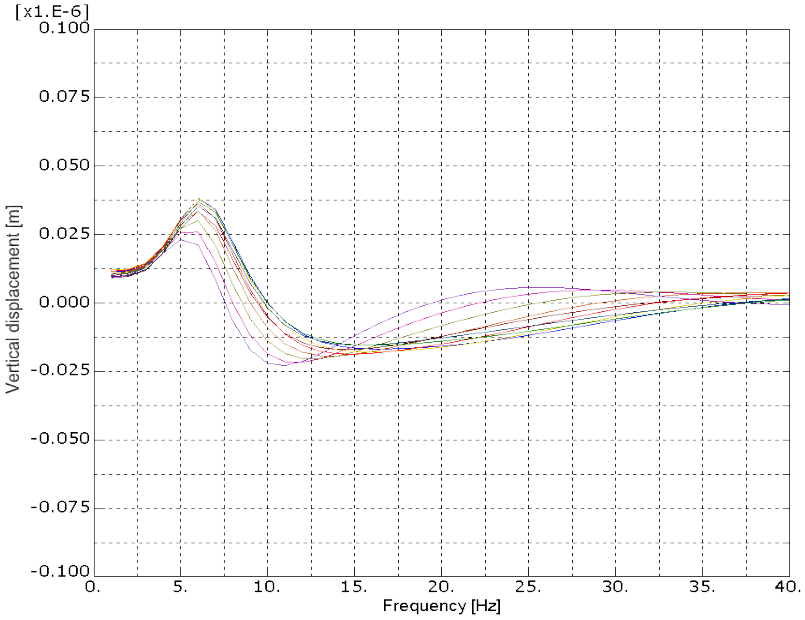

Figure A.20: Displacement vs frequency, 150 pillars.

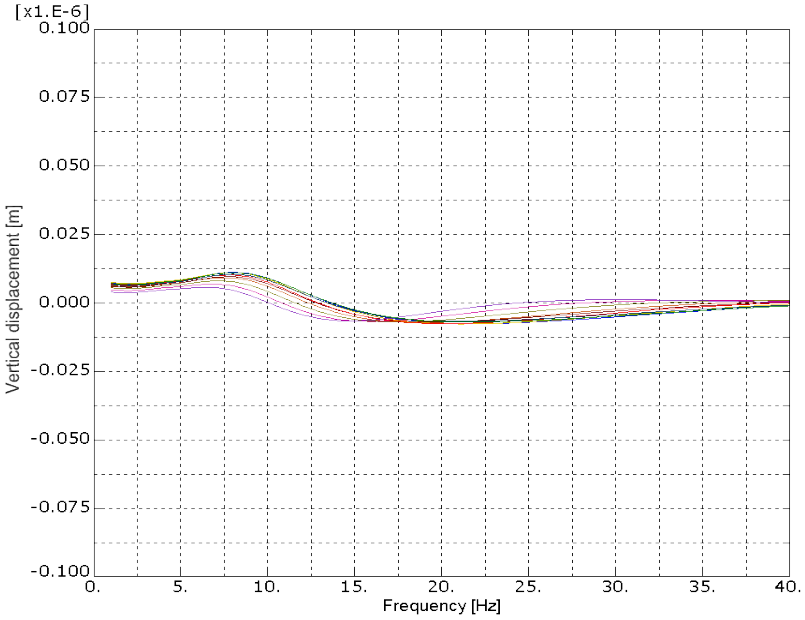

Figure A.21: Displacement vs frequency, 600 pillars.

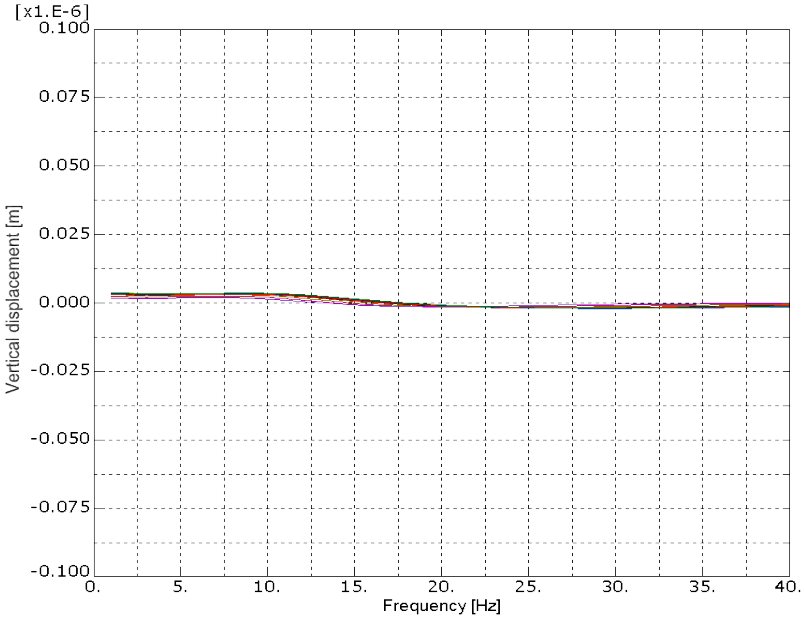

Figure A.22: Displacement vs frequency, 3500 pillars.

Pillars and floor thickness

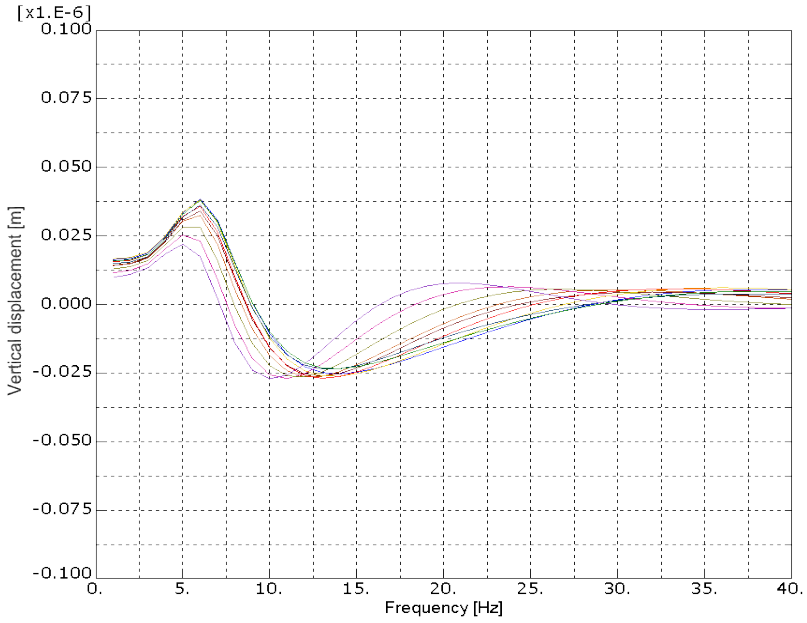

Figure A.23: Displacement vs frequency, floor thickness of 500 mm, 150 pillars.

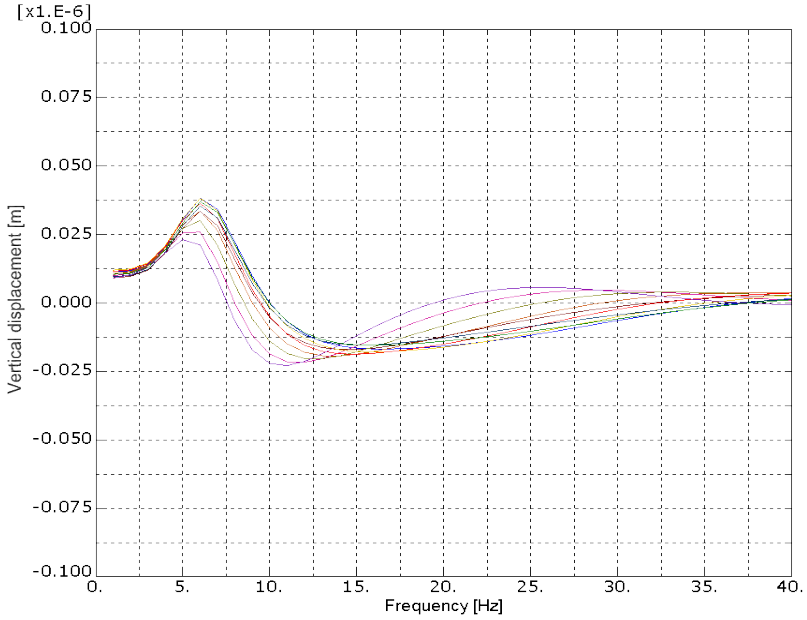

Figure A.24: Displacement vs frequency, floor thickness of 700 mm, 150 pillars.

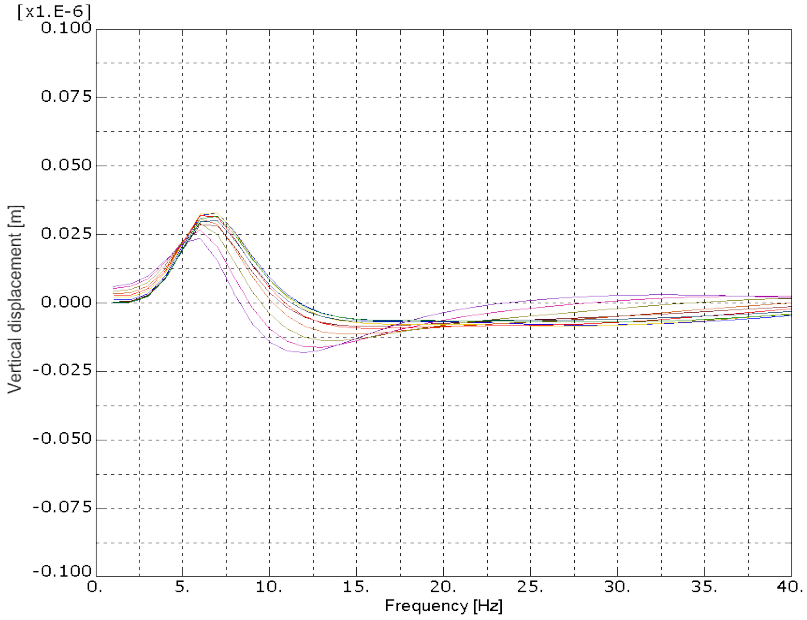

Figure A.25: Displacement vs frequency, floor thickness of 1000 mm, 150 pillars.

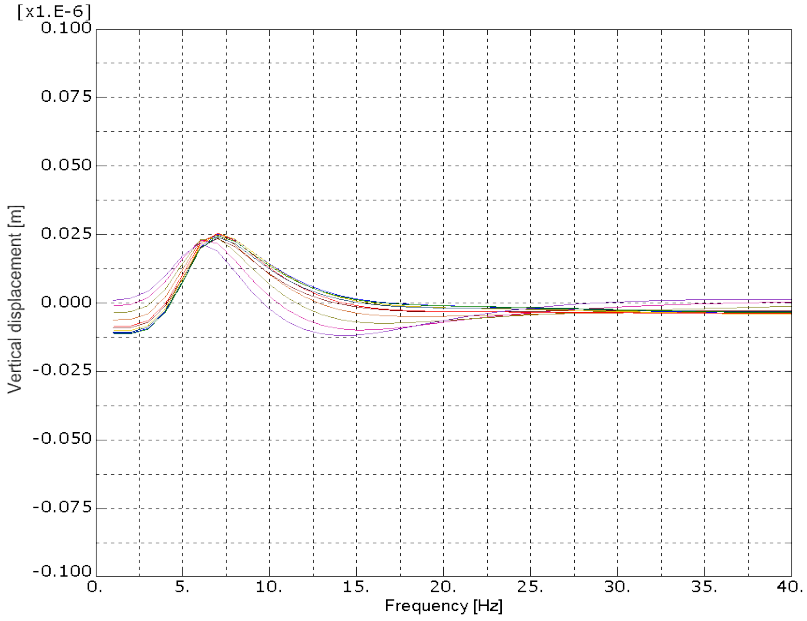

Figure A.26: Displacement vs frequency, floor thickness of 1400 mm, 150 pillars.

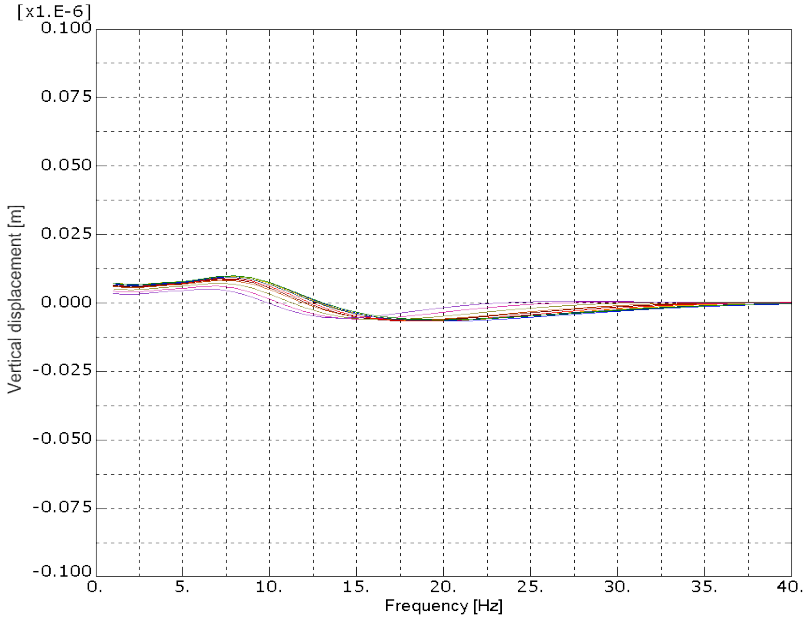

Figure A.27: Displacement vs frequency, floor thickness of 500 mm, 600 pillars.

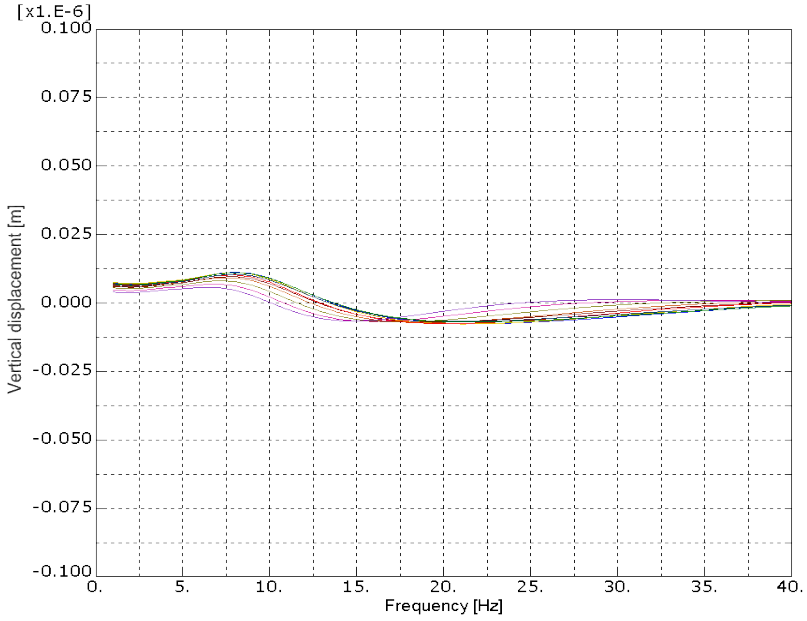

Figure A.28: Displacement vs frequency, floor thickness of 700 mm, 600 pillars.

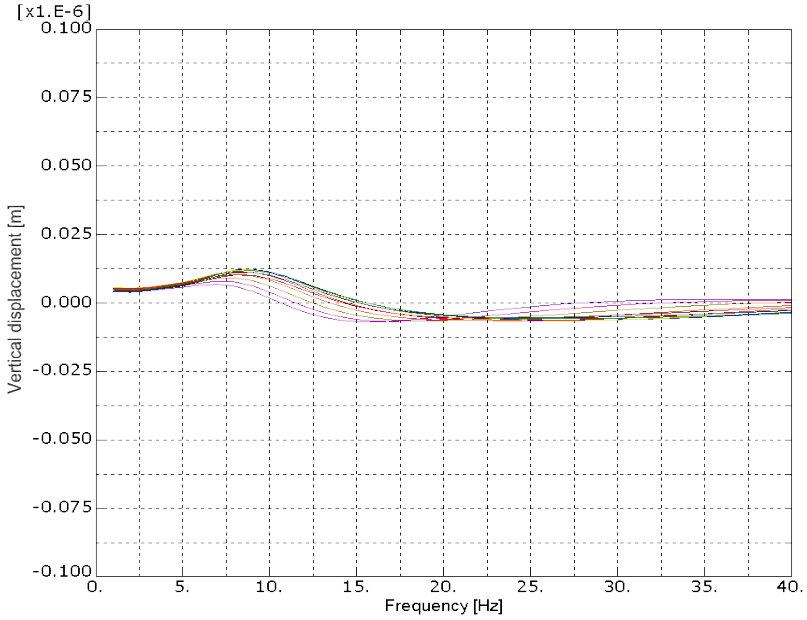

Figure A.29: Displacement vs frequency, floor thickness of 1000 mm, 600 pillars.

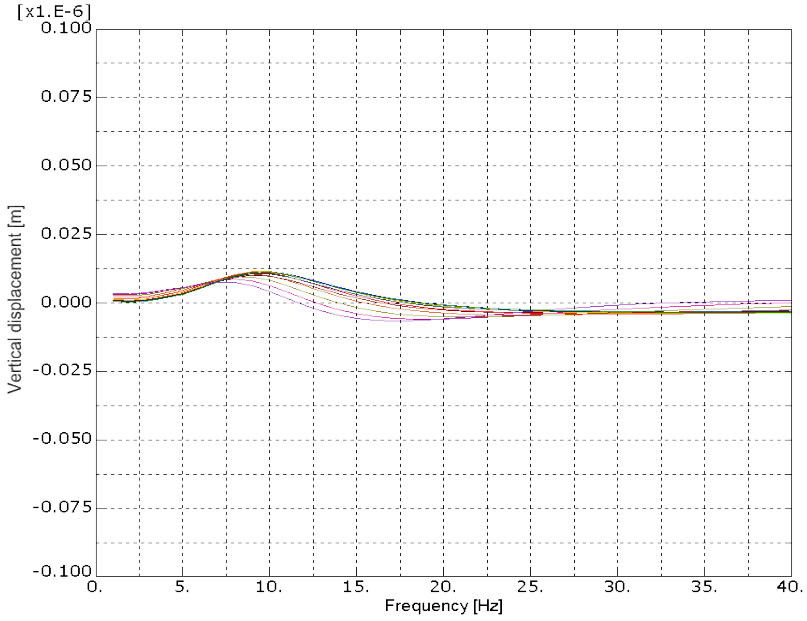

Figure A.30: Displacement vs frequency, floor thickness of 1400 mm, 600 pillars.

Divided floor

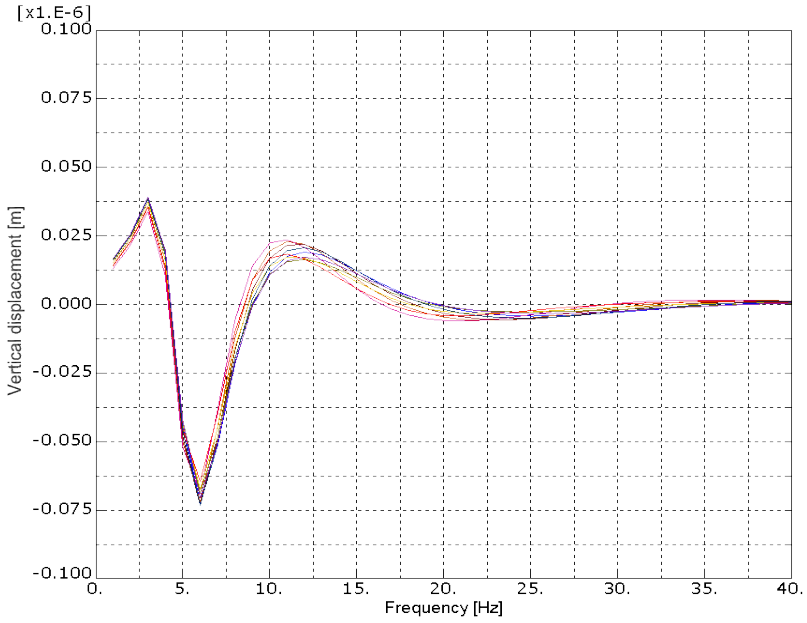

Figure A.31: Displacement vs frequency, original floor, load position 1.

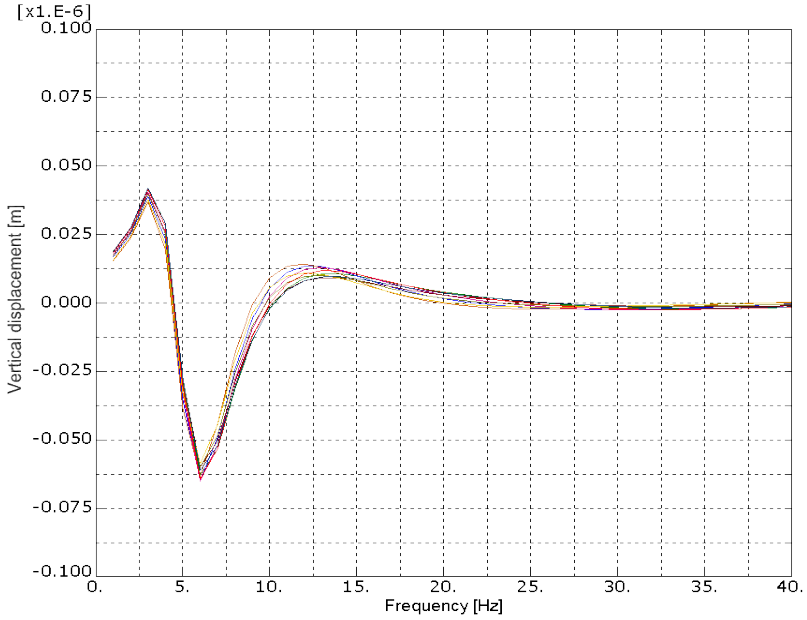

Figure A.32: Displacement vs frequency, original floor, load position 2.

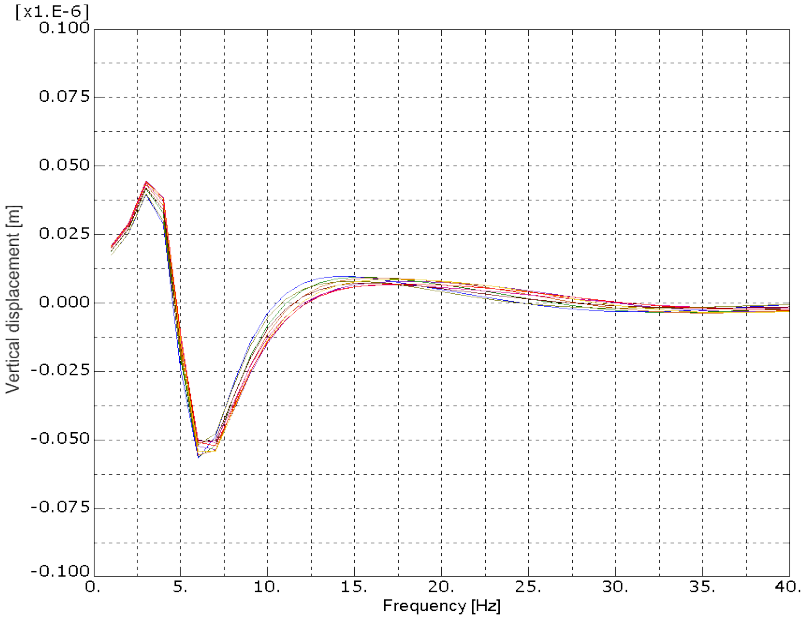

Figure A.33: Displacement vs frequency, original floor, load position 3.

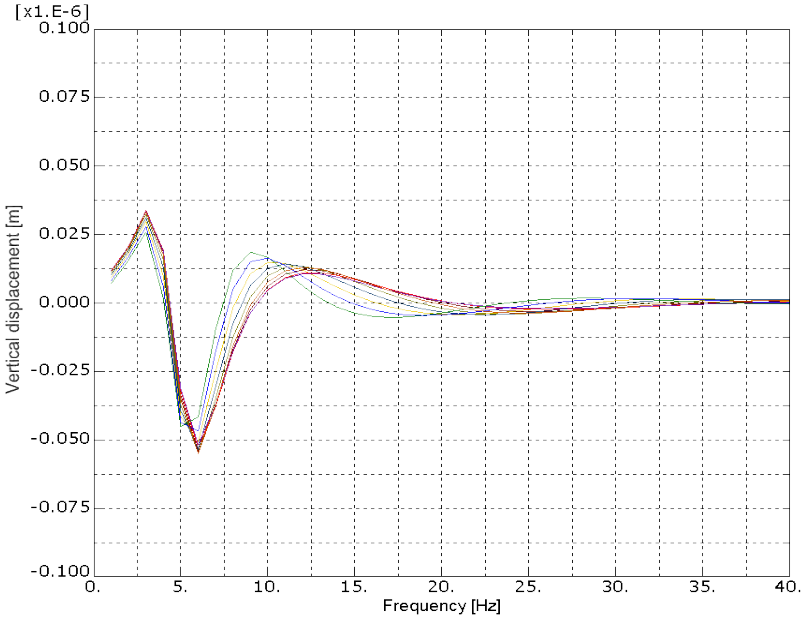

Figure A.34: Displacement vs frequency, divided floor, load position 1.

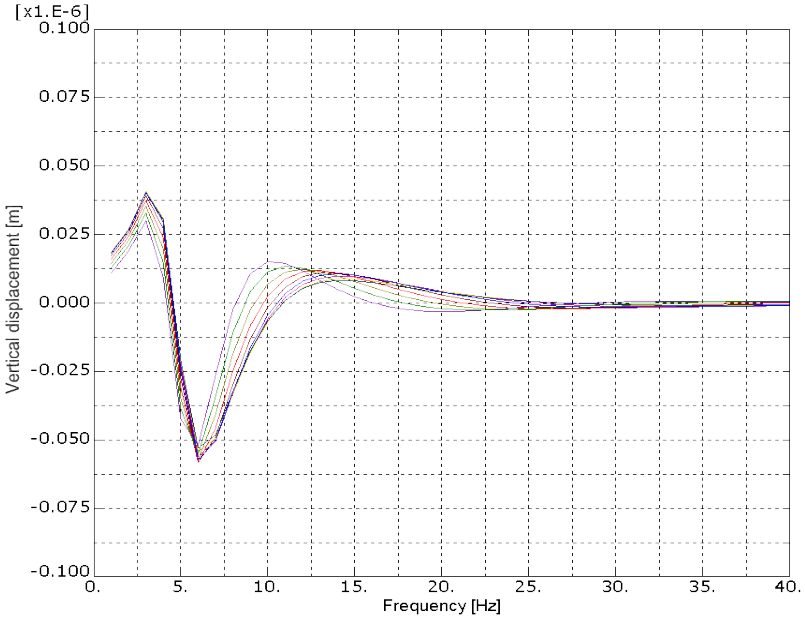

Figure A.35: Displacement vs frequency, divided floor, load position 2.

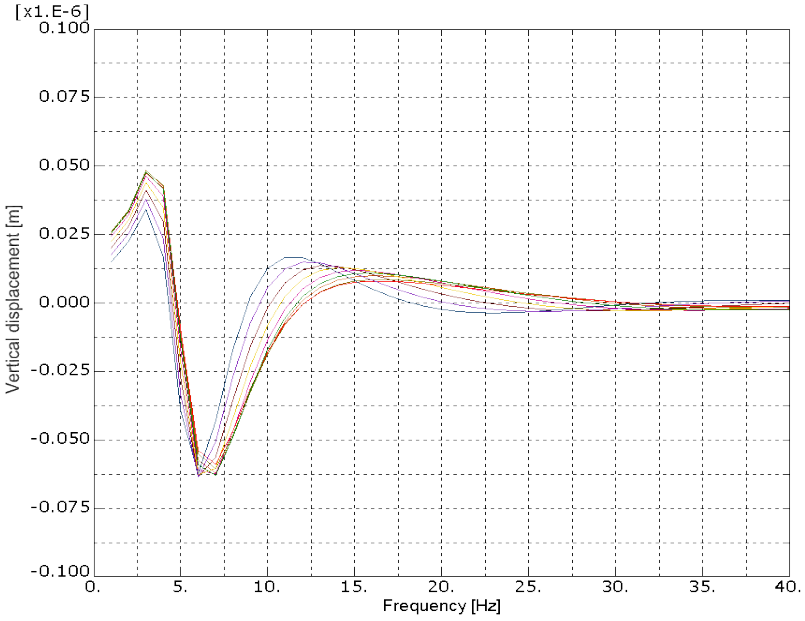

Figure A.36: Displacement vs frequency, divided floor, load position 3.

Divided floor and pillars

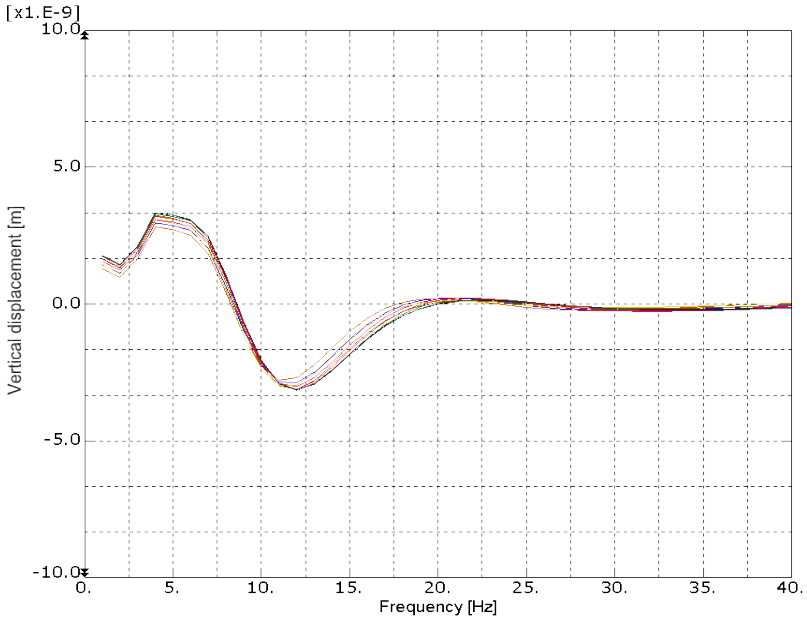

Figure A.37: Displacement vs frequency, original floor, load position 1, 600 pillars.

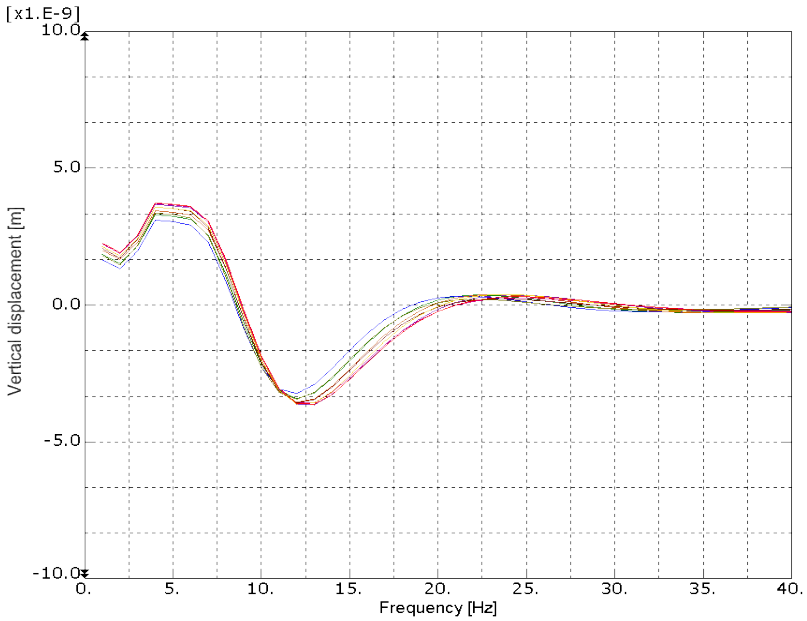

Figure A.38: Displacement vs frequency, original floor, load position 2, 600 pillars

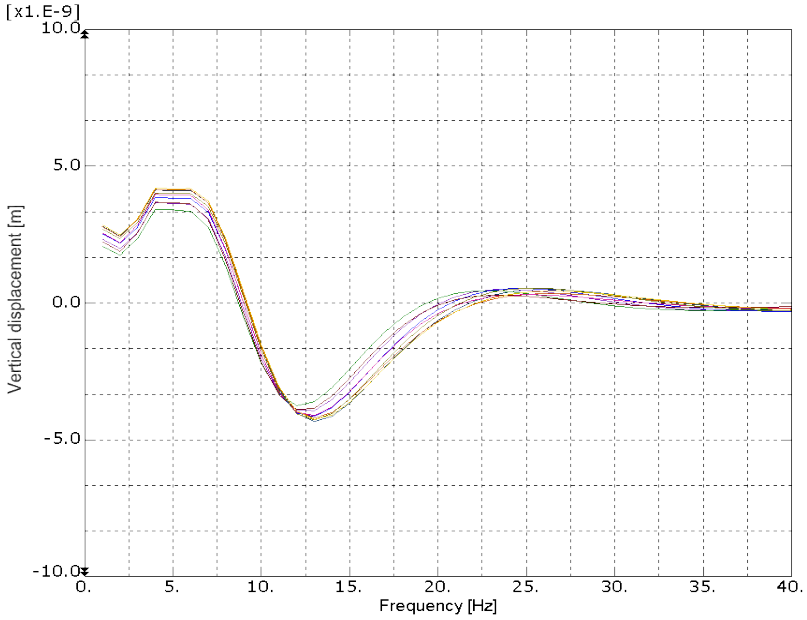

Figure A.39: Displacement vs frequency, original floor, load position 3, 600 pillars

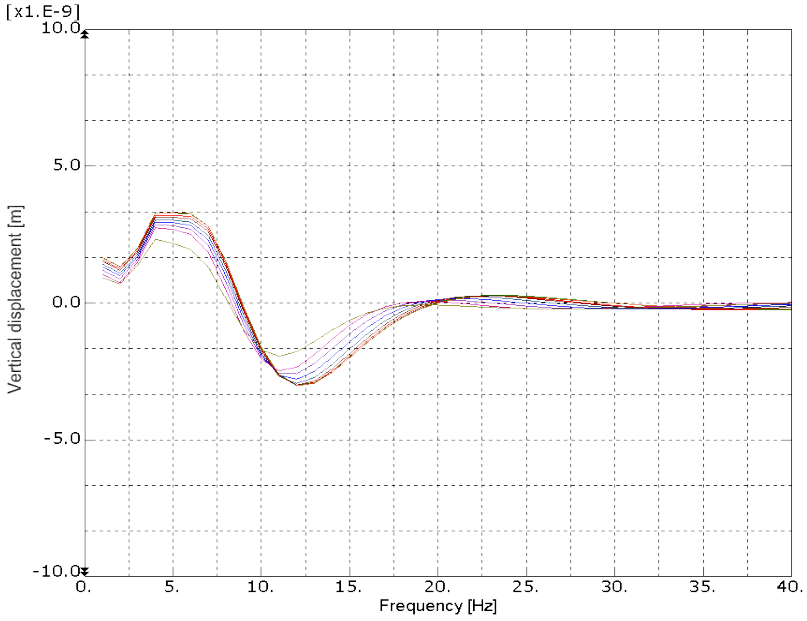

Figure A.40: Displacement vs frequency, divided floor, load position 1, 600 pillars

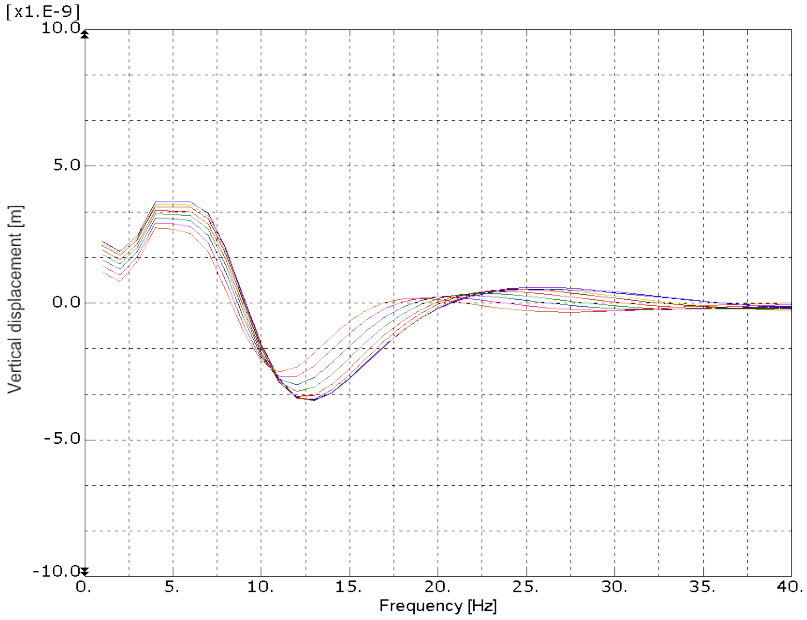

Figure A.41: Displacement vs frequency, divided floor, load position 2, 600 pillars

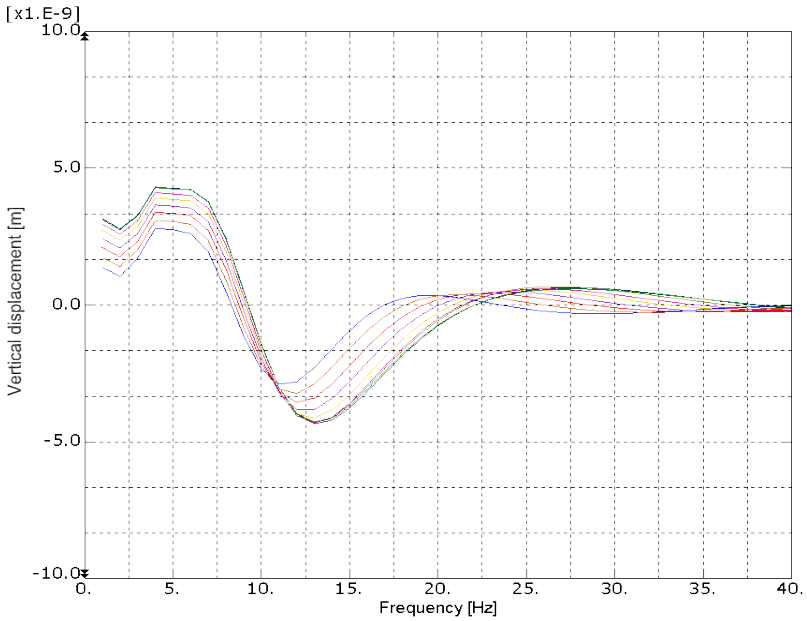

Figure A.42: Displacement vs frequency, divided floor, load position 3, 600 pillars